http://www.icae.jp

Newsletter on Atmospheric Electricity

Vol. 27 • No 1 • May 2016

INTERNATIONAL COMMISSION ON ATMOSPHERIC ELECTRICITY (IAMAS/IUGG)

AMS COMMITTEE ON ATMOSPHERIC ELECTRICITY

AGU COMMITTEE ON ATMOSPHERIC AND SPACE ELECTRICITY

EUROPEAN GEOSCIENCES UNION

SOCIETY OF ATMOSPHERIC ELECTRICITY OF JAPAN

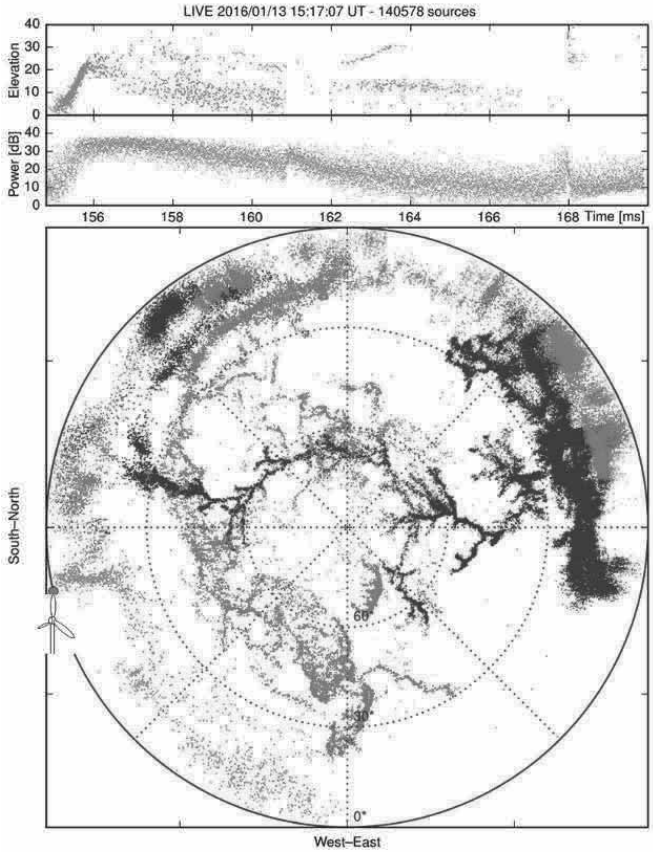

Comment on the photo above: **A complex winter IC lightning flash that triggered an upward lightning discharge from a wind turbine at Uchinada, Japan as seen by LIVE (Lightning Imaging via. VHF Emission). In the still image, the beginning of the flash is shown in blue, the middle green, and the end red. The majority of the lightning channels were produced by negative breakdown, with several channels growing at the same time. VHF emission from this type of growth tends to interfere with itself, making both interferometric and time-of-arrival mapping more difficult. The upward flash began at 158.4 ms (green in the still figure), and produced bright, continuous VHF emission. Study of this and other Japanese winter lightning flashes is ongoing. The complexity of this flash is not unusual in comparison to other winter flashes, showing that there is still quite a lot to learn about Japanese winter lightning. Video is provided by Michael Stock, RAIRAN Pte. Ltd., Japan.**

ANNOUNCEMENTS

LIS Very High Resolution Gridded Lightning Climatology Data Sets

The LIS 0.1 Degree Very High Resolution Gridded Climatology data collection consist of gridded climatologies of total lightning flash rates seen by the Lightning Imaging Sensor (LIS) onboard of the Tropical Rainfall Measuring Mission (TRMM) satellite. The Very High Resolution Gridded Lightning Climatology Collection consists of five datasets including the full (VHRFC), monthly (VHRMC), diurnal (VHRDC), annual (VHRAC), and seasonal (VHRSC) lightning climatologies. These gridded climatologies include annual mean flash rate, mean diurnal cycle of flash rate with 24 hour resolution, and mean annual cycle of flash rate with daily, monthly, or seasonal resolution. All datasets are in 0.1 degree spatial resolution, where the mean annual cycle of flash rate datasets (i.e., daily, monthly or seasonal) have both 49-day and 1 degree boxcar moving average to remove diurnal cycle and smooth regions with low flash rate to make the results more robust.

All the datasets can be navigated in your browser using GoogleEarth plugin at http://lightning.nsstc.nasa.gov/data/data_lis-vhr-climatology.html.

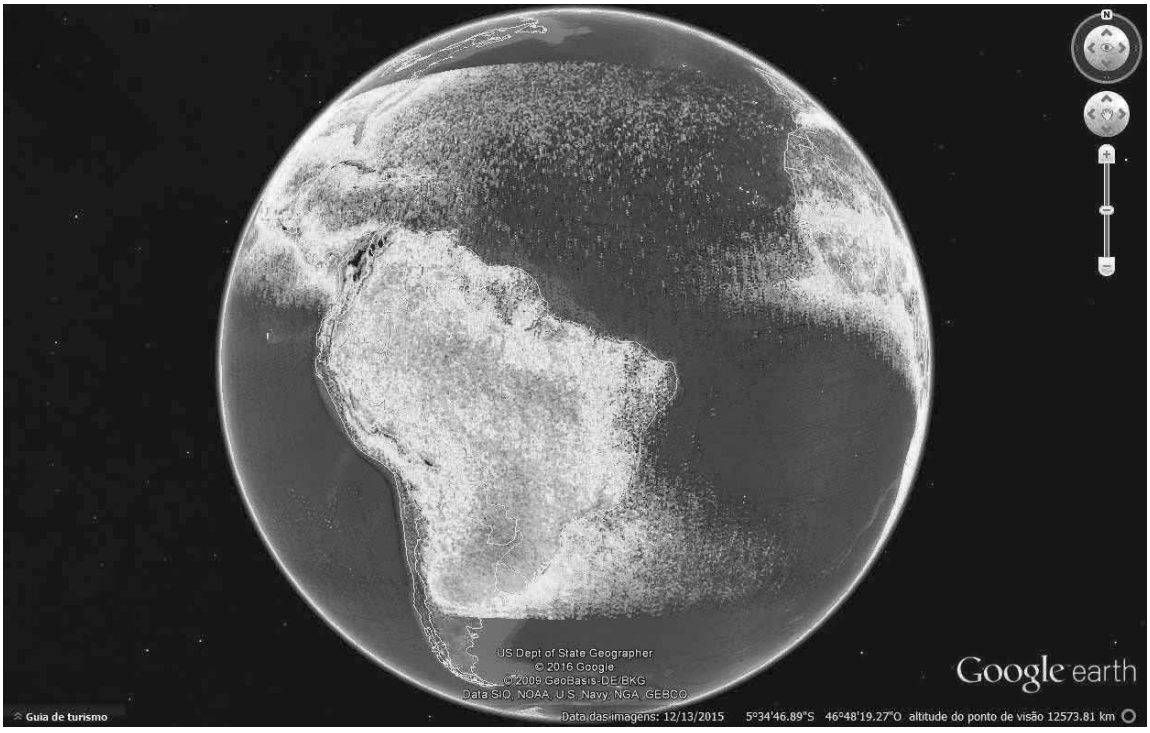

More information about each dataset in this collection is provided on the landing page at the appropriate DOI link below and the recent article in the *Bulletin of American Meteorological Society* by Albrecht et al. (currently in the *Early Online Releases*).

ANNOUNCEMENTS

Albrecht, R., S. Goodman, D. Buechler, R. Blakeslee, and H. Christian. 2016. LIS 0.1 Degree Very High Resolution Gridded Lightning Climatology Data Collection. Data sets available online [https://ghrc.nsstc.nasa.gov/pub/lis/climatology/LIS/] from the NASA Global Hydrology Resource Center DAAC, Huntsville, Alabama, U.S.A. doi: http://dx.doi.org/10.5067/LIS/LIS/DATA306.

New Books

Fundamentals of Lightning

Cambridge University Press, 257 p., 2016, ISBN: 9781107072237, V.A. Rakov
http://www.cambridge.org/us/academic/subjects/earth-and-environmental-science/atmospheric-science-and-meteorology/fundamentals-lightning?format=HB

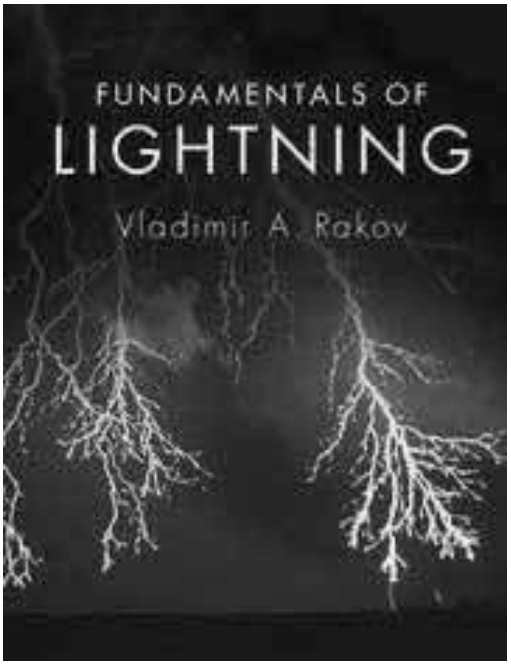

Description
This new book provides a focused set of topics suitable for advanced undergraduate or graduate courses on lightning. It presents the current state of the art in lightning science including areas such as lightning modeling, calculation of lightning electromagnetic fields, electromagnetic methods of lightning location, and lightning damaging effects and protective techniques. Pedagogical features designed to facilitate class learning include end-of-chapter summaries, further reading suggestions, questions and problems, and a glossary explaining key lightning and atmospheric electricity terms. A selection of appendices are provided at the end of the book, which include detailed derivations of exact equations for computing electric and magnetic fields produced by lightning. Designed for a single-semester course on lightning and its effects, and written in a style accessible to technical non-experts, this book will also be a useful,

up-to-date reference for scientists, engineers and practitioners who have to deal with lightning in their work.

Table of Contents

Dedication
Preface
1. Types of lightning discharges and lightning terminology
2. Incidence of lightning to areas and structures
3. Electrical structure of thunderclouds
4. Properties of the downward negative lightning discharge to ground
5. Calculation of lightning electromagnetic fields
6. Modeling of lightning processes
7. Measurement of lightning electric and magnetic fields
8. Electromagnetic methods of lightning location
9. Lightning damaging effects and protective techniques
Appendix 1. How is lightning initiated in thunderclouds?
Appendix 2. Reconstruction of sources from measured electrostatic field changes
Appendix 3. Derivation of exact equations for computing lightning electric and magnetic fields
Appendix 4. Compact intracloud discharges (CIDs)
Appendix 5. Is it true that lightning never strikes the same place twice?
Appendix 6. Is it possible to use lightning as an energy source?
Appendix 7. Lightning safety
Appendix 8. Lightning makes glass
Appendix 9. Bibliography on triggered lightning experiments and natural lightning observations at Camp Blanding, Florida (1995–2014)
Glossary
References
Index

Electromagnetic Computation Methods for Lightning Surge Protection Studies

Wiley-IEEE Press, 320 p., 2016, ISBN: 978-1-118-27563-4, Y. Baba and V.A. Rakov
http://www.wiley.com/WileyCDA/WileyTitle/productCd-1118275632,subjectCd-EE33.html

ANNOUNCEMENTS

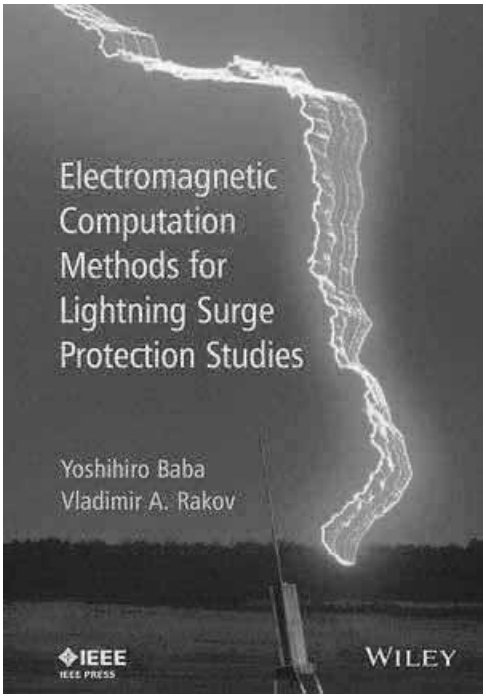

Description

Presents current research into electromagnetic computation theories with particular emphasis on Finite-Difference Time-Domain Method

This book aims at providing an introduction to electromagnetic computation methods with a focus on the finite-difference time-domain (FDTD) method for lightning surge protection studies. The FDTD method is based on a simple procedure, and therefore its programming is relatively easy. Also, it is capable of treating complex geometries and inhomogeneities, as well as incorporating nonlinear effects and components. This book is composed of four chapters. In Chapter 1, an overview of lightning electromagnetic field and surge computations is given, and the existing electromagnetic computation methods are introduced. In Chapter 2, it is explained how lightning discharges are generated. Salient features of lightning return-stroke current and those of lightning electric and magnetic fields are discussed. Also, mathematical expressions for calculating lightning return-stroke electric and magnetic fields are presented. Further, lightning surges in electric power and telecommunication systems are described, and measures for protecting these systems against lightning surges are reviewed. In Chapter 3, update equations for electric and magnetic fields used in FDTD computations in the 3D Cartesian coordinate system and in the 2D cylindrical coordinate system are presented. Also, representations of lumped sources, lumped linear circuit elements, such as a resistor, an inductor and a capacitor, and a lumped nonlinear element are described. Further, representations of thin wire and lightning channel are discussed. Finally, in Chapter 4, representative applications of the FDTD method to lightning electromagnetic field and surge simulations are reviewed. In Appendix, an example of FDTD program written in C programming language for computing lightning electric and magnetic fields in the 3D Cartesian coordinate system is provided. This book is suitable for senior undergraduate and graduate students specializing in electrical engineering, as well as for electrical engineers and researchers, who are interested in lightning surge protection studies.

ANNOUNCEMENTS

Table of Contents

Preface
1. Introduction
1.1. Historical Overview of Lightning Electromagnetic-Field and Surge Computations
1.2 Overview of Existing Electromagnetic Computation Methods
1. Lightning
2.1. Introduction
2.2. Thundercloud
2.3 Lightning Discharges
2.4. Lightning Electromagnetic Fields
2.5. Lightning Surges
2.6. Lightning Surge Protection
3. The Finite-Difference Time Domain Method for Solving Maxwell's Equations
3.1. Introduction
3.2. Finite-Difference Expressions of Maxwell's Equations
3.3. Subgridding Technique
3.4. Absorbing Boundary Conditions
3.5. Representation of Lumped Sources and Lumped Circuit Elements
3.6. Representation of Thin wire
3.7. Representation of Lightning Return-Stroke Channel
3.8. Representation of Surge Arresters
4. Applications to Lightning Surge Protection Studies
4.1. Introduction
4.2. Electromagnetic Fields at the Top of a Tall Building Associated with Nearby Lightning Return Strokes
4.3. Influence of Strike Object Grounding on Close Lightning Electric Fields
4.4. Simulation of Corona at Lightning-Triggering Wire: Current, Charge Transfer, and Field Reduction Effect
4.5. On the Interpretation of Ground Reflections Observed in Small-Scale Experiments Simulating Lightning Strikes to Towers
4.6. On the Mechanism of Attenuation of Current Waves Propagating along a Vertical Perfectly Conducting Wire above Ground: Application to Lightning
4.7. FDTD Simulation of Lightning Surges on Overhead Wires in the Presence of Corona Discharge
4.8. FDTD Simulation of Insulator Voltages at a Lightning-Struck Tower Considering the Ground-Wire Corona
4.9. Voltages Induced on an Overhead Wire by Lightning Strikes to a Nearby Tall Grounded Object
4.10. 3D-FDTD Computation of Lightning-Induced Voltages on an Overhead Two-Wire Distribution Line
4.11. FDTD Simulations of the Corona Effect on Lightning-Induced Voltages
4.12. FDTD Simulation of Surges on Grounding Electrodes Considering Soil Ionization
References

ANNOUNCEMENTS

Appendix: 3D-FDTD Program in C
Index

CONFERENCES

ICLP 2016

The 33rd International Conference on Lightning Protection (ICLP) will be held in Estoril, Portugal during 25-30 September, 2016. For detail, please visit http://iclp2016.org/.

Workshop on Terrestrial Gamma-ray Flashes

The University of Alabama in Huntsville (UAH) and its Center for Space Plasma and Aeronomic Research (CSPAR) will host a three daylong workshop on Terrestrial Gamma-ray Flashes on 13-15 July 2016. (This is a change from the first announcement, due to a conflict with another conference.) The workshop will be informal and designed to encourage discussions. Submissions are invited on TGFs, including observations and theory, future instruments, other atmospheric high-energy radiation phenomena, and related thunderstorm and lightning science. Additional information is available at http://tgf2016.uah.edu/.

The date for early registration and abstracts is June 13.

Open call for nominations for the prestigious ICLP Berger and Golde awards

We are pleased to announce that the call for nominations for the prestigious ICLP Berger and Golde awards is now open. The scientific committee of the ICLP bestows these awards upon four scientists:

Karl Berger Award
For distinguished achievements in the science and engineering of lightning research, developing new fields in theory and practice, modeling and measurements.

Rudolf Heinrich Golde Award

ANNOUNCEMENTS

For distinguished achievements in the science and engineering of lightning protection, developing safe technologies or innovative uses and applications.
Please send in your nominations before August 15th, 2016 to Prof. Joan Montanyà (montanya@ee.upc.edu) containing:
1) the award for which the nomination is given, Berger or Golde,
2) a one or two-line proposed citation, and
3) a description of the technical achievements of the nominee.

Once the nominations are in, a distinguished panel of judges consisting of the previous recipients of these awards will rank the nominees according to their standing in the research community and for their contributions to the field. Based on this ranking, the Awards Committee will select the recipients of the two awards.

Authors' clarification to "When does the lightning attachment process actually begin?" and "Attachment process in subsequent strokes and residual channel luminosity between strokes of natural lightning" by M.D. Tran and V.A. Rakov

The so-called faintly luminous formations (FLFs) have been recorded in the single, pre-return-stroke frame by a high-speed video camera Phantom V310 and presented in references 1 and 2. Subsequently we found that some of the FLFs might have been affected by the so-called parasitic light sensitivity (PLS) of the camera, which is associated with the imperfect shielding of pixel-value storage nodes and their relatively long read-out time. The effect amounts to the "bleeding" of return-stroke light to the immediately-preceding (pre-return-stroke) frame. The intensity of resultant camera artifact in the pre-return-stroke frame is only 10-4 to 10-3 of the return-stroke intensity, but it can materially influence and even overwhelm the actual FLF (if any) in the pre-return-stroke frame. Thus, the interpretation of FLFs in references 1 and 2 and the results of striking-distance analysis in reference 1 cannot be viewed as reliable. On the other hand, the results concerning the leader speed/connection rate profiles and estimates of average electric field between the leader tip and ground in reference 1, as well as the study of residual channel luminosity between strokes and estimates of channel current ahead of the subsequent-leader front in reference 2 are not affected by PLS.

It is worth noting that there exist FLF images recorded by high-speed video cameras in two or more consecutive frames. Examples are found in Figs. 2 and 5 in reference 3 (captured with a Photron FASTCAM SA5 camera operated at 300,000 frames per second) and in Fig. 1 in reference 4 (captured with a Phantom V711 camera operated at 10,000 frames per second with exposure time of 40 μs). It is not clear if those multiple-frame FLF images could be materially influenced by PLS.

We thank Alexander Kostinskiy who was the first to attract our attention to the existence of PLS in various framing cameras and encouraged us to perform laboratory tests of the Phantom V310 using laser and other light sources. We also appreciate helpful cooperation of Radu Corlan of Vision Research, the manufacturer of Phantom V310.

References

1. Tran M.D. and V.A. Rakov. 2015. When does the lightning attachment process actually begin? J. Geophys. Res. Atmos., 120, 6922–6936.

2. Tran M.D. and V.A. Rakov. 2015. Attachment process in subsequent strokes and residual channel luminosity between strokes of natural lightning. J. Geophys. Res. Atmos., 120, 12,248–12,258.

3. Xie S., F. D'Alessandro, W. Chen, J. He, and H. He. 2013. Attachment processes and influencing factors in competition tests under switching impulse voltages. IEEE Trans. Plasma Sci., 41(7), 1773–1780.

4. Jiang, R., X. Qie, Z. Wang, H. Zhang, G. Lu, Z. Sun, M. Liu, and X. Li. 2015. Characteristics of lightning leader propagation and ground attachment. J. Geophys. Res. Atmos., 120, 11,988–12,002.

RESEARCH ACTIVITY BY INSTITUTIONS

Atmospheric Electricity Group (ELAT), INPE, Brazil

We are investigating the lightning attachment process to common buildings (Fig. 1). We analyze upward connecting leaders induced by some downward negative lightning flashes that strikes an ordinary residential building located in São Paulo City, Brazil. With high-speed cameras placed at a distance of 200m (Fig. 2), running at tens of thousands images per second, details of the connection process are studied (ratio between velocities, striking distances, final jump discharges, etc.). Considering that there are almost no observational data of lightning attachment to common structures or buildings (under 60 m - present in almost every city), we believe that this study will contribute to the understanding of lightning attachment.

Fig. 1 Negative cloud-to-ground flash striking one of the buildings under observation.

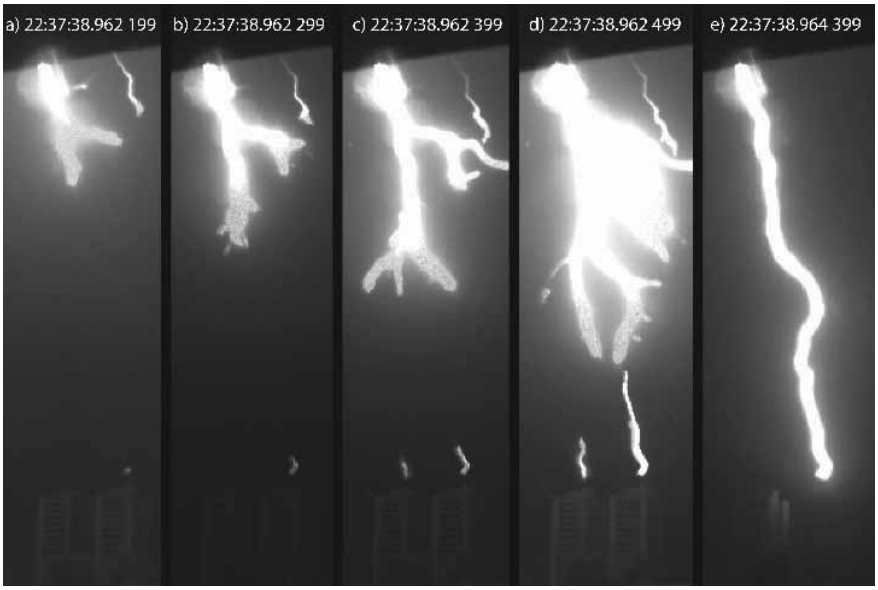

Fig. 2 Sequence of video images showing the initiation and development of an upward connecting leader and two unconnected upward leaders on February 9th, 2014.

Bristol Industrial and Research Associates Limited (Biral)

Alec Bennett

A new thunderstorm detector was developed by Biral in 2013, which detects all forms of lightning within ~100 km, using the electrostatic component of the E-field change associated with the flash. Strong E-field changes due to wind-blown space charge and charged hydrometeors present at the site are also used for thunderstorm warning. An integrated low frequency radio direction finder is used to provide lightning bearing. Whilst the instrument, referred to as the BTD-300, is

designed for commercial use as a standalone thunderstorm warning system, the raw 100 Hz antenna displacement current data are continuously recorded at Biral's instrument development sites near Bristol, UK. These data provide research opportunities in areas such as lightning quasi-electrostatic field change, near-surface space charge variability and hydrometeor charge. The instrument's sensitivity and 1-45 Hz passband also allows Schumann resonances to be detected during electrically quiet periods. The site's proximity to 130m tall wind turbines (10 km) and a 293m TV mast (40 km) is used to investigate induced lightning flashes. Recent assessment indicates that flashes suspected to be self-initiated by these structures under otherwise non-lightning producing Cumulonimbus are readily detected electrostatically but do not always produce sufficient low frequency radiation to be detected by VLF/LF lightning location networks.

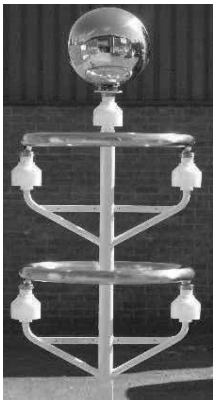

Fig. 1 The BTD-300 thunderstorm detector. The spherical and toroidal antennas are used to measure the electrostatic component of the E-field change due to lightning, wind-blown space charge and hydrometeor charge. The multiple antennas aid discrimination of different charge sources.

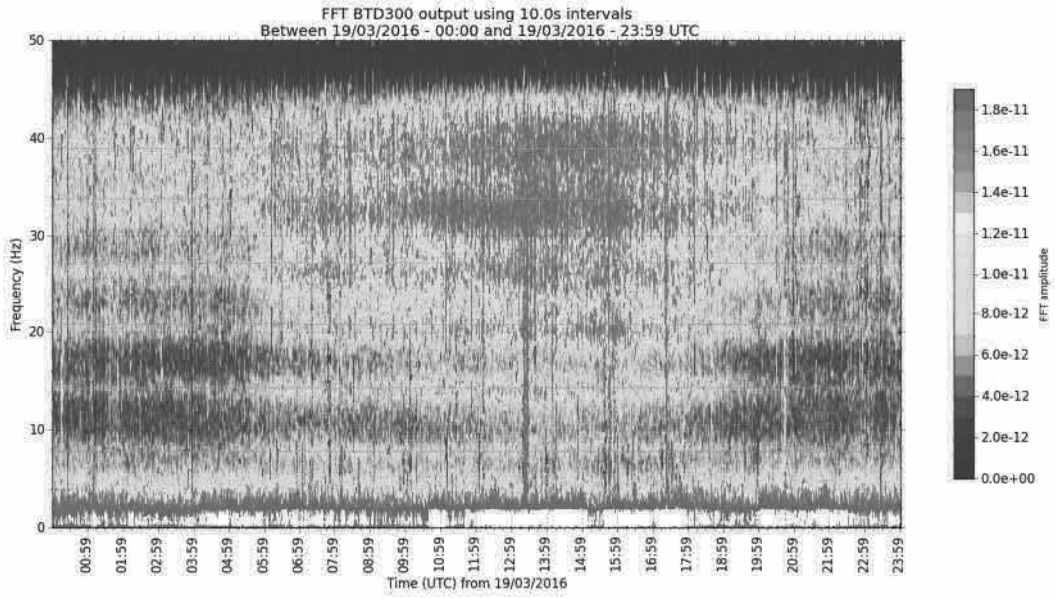

Fig. 2 Example of six Schumann resonances detected by the BTD-300 over 24 hours (expected frequencies shown as horizontal grey lines). The plot shows an enhancement between 06-19 UTC, which corresponds to local daytime. The higher amplitude variability below ~4 Hz represents the turbulent movement of near-surface space charge.

RESEARCH ACTIVITY BY INSTITUTIONS

Colorado State University

Doug Stolz, Steven Rutledge, Jeffrey Pierce and Sue van den Heever

Previous studies have implicated multiple environmental factors (e.g., CAPE, cloud condensation nuclei, warm cloud depth, shear, and ambient relative humidity) for influencing lightning variability on global/regional scales as well as between seasons. Our group's latest efforts on this front have been focused on determining the relative influence of each of the aforementioned factors on total lightning density and radar reflectivity from TRMM climatology. In our statistical analyses of this problem, we find that cloud condensation nuclei (CCN) account for the largest individual contribution to the aforementioned variability (holding other inputs constant) in an eight-year subset of the convective cloud population observed by the TRMM satellite. Notably, up to 81% of the variability in total lightning density can be approximated by a linear combination of the chosen environmental factors using various weightings derived from multiple linear regression. Given the strong relationship between lightning and mixed-phase radar reflectivity documented in the literature to date, we find similar results when investigating global/regional variations of average 30 dBZ echo top height. These results are shown to be consistent over the global TRMM domain, between continents and oceans, between hemispheres, as well as over smaller-scale regions encompassing the Amazon and Congo River basins. Manuscripts detailing these studies are currently under review in the Journal of Geophysical Research - Atmospheres and the Journal of Atmospheric Sciences.

Karly Reimel, Steven Rutledge, Steve Miller (CIRA) and Dan Lindsay (CIRA)

In preparation for the launch of GOES-R and the Geostationary Lightning Mapper (GLM), we are carrying out case study analyses of severe storms in the Colorado Lightning Mapping Array(COLMA) region. By combining radar, satellite, COLMA, and National Lightning Detection Network (NLDN) data, a similar dataset to the one GOES-R and GLM will provide can be used. The goal of this work is to determine a relationship between lightning characteristics and the dynamics of severe storms. Flash rate, flash size, flash location, flash polarity, and intra-cloud to cloud-to-ground flash ratios, are being considered. Case study analyses will demonstrate the potential uses of GLM and will help set expectations for the instrument's performance, which can be used in the calibration/validation period of the instrument.

Brody Fuchs, Eric Bruning (Texas Tech), Steven Rutledge, Paul Krehbiel (NMIMT) and Bill Rison (NMIMT)

Recent efforts have focused on investigating the variability of thunderstorm processes and lightning characteristics in different thermodynamic environments in the United States. Storms exhibit variability in lightning flash rates and charge structures coincident with thermodynamic variability. We have used an automated algorithm that clusters high-resolution lightning mapping data into lightning flashes to produce multiyear climatologies of flash densities and flash characteristics in multiple regions of the United States with LMA networks. From these climatologies, we discovered a large discrepancy in total flash density and the ratio of cloud flashes to ground flashes between the LMA and corresponding satellite estimates in northeast Colorado. Further investigation revealed that the lightning flash characteristics in the region were

substantially different from those in other regions of study. Of particular importance to satellite comparisons are the smaller spatial extent and lower initiation altitude of most flashes. Both of these factors may make optical detection of lightning by satellites more difficult. The northeastern Colorado region is characterized by much higher cloud base heights than the other regions of study, which is hypothesized to favor mixed-phase precipitation over warm-phase precipitation. This permits larger amounts of supercooled water in the mixed-phase region and leads to anomalous charging of precipitation ice, which is potentially responsible for the unusual lightning characteristics observed in the region. These differences prompted us to consider the possibility of other regions of the globe with similar thermodynamic environments, which we hypothesize may have similar lightning detection issues. This would result in an alteration of the global lightning flash climatologies.

Weixin Xu, Wenjuan Zhang, and Steven Rutledge

Another component at CSU is a study concerning the relationships between Lightning and Tropical Cyclone Intensity Change. Previous studies suggest that lightning activity could be an indicator of Tropical Cyclones (TC) intensity change but their relationships vary greatly and at times contradictory. So far, most TC lightning studies were based on measurements from the NLDN, WWLLN, and similar ground-based networks. While NLDN observes total lightning within a few hundred kilometers of land, WWLLN detects a smaller fraction of the TC lightning, mostly CG lightning. Several studies have shown the importance of total lightning for TC intensification study and forecast. Our research leverages the 16-yr total lightning data recorded by TRMM LIS to investigate TC lightning characteristics, lightning-TC intensity change relationship, and relations between TC lightning and environmental factors. Of the six basins examined, the Atlantic and the Northern Indian Ocean have the highest TC lightning density where environmental wind shear is also the greatest. It is interesting that North West Pacific TCs are the least electrified given the underlying warm oceans. Lightning activity increases dramatically when TCs move close to land possibly due to TC-aerosol interaction (Fig. 1a). Lightning density increases as SST increases but decreases after SST becomes warmer than 30 C. Decreased (elevated) lightning density in the inner core (outer rainband) are observed 24h prior to TC intensification (Fig. 1b), which is similar to the CG lightning patterns reported by recent statistical studies using WWLLN data (DeMaria et al. 2012). Similar relationships between 30 dBZ echo-top height (a good indicator of intense convection) and TC intensity change are also found. However, convective depth, as indicated by 20 dBZ echo-top height and IR brightness temperature, show a positive relationship to future TC intensity change (Fig. 1c). These results suggest that tall precipitation (deep convection) cores can promote TC intensification possibly through latent heat release and vortex stretching, consistent with previous studies (Kelly et al. 2004). Lightning-producing intense convection may generate negative effects on TC intensification due to development of cold pools, downdrafts, and its underlying stronger shear environment. Both lightning density and convective depth increase substantially following (24 h) TC intensification, suggesting vigorous convection with lightning may be a response to TC intensification more than a leading signal as proposed by previous researchers. Molinari et al. (1999) suggested that the sign of the intensity change may be dependent on the prior intensity change, where weakening or slowly intensifying TCs are likely to intensify

after a lightning burst in the IC. Nevertheless, our statistics based on TRMM LIS shows that the negative relationship between lightning density and TC intensity change stays the same when TCs are categorized by prior intensity change.

We also examined the six hourly evolution of CG lightning, TC intensity, environments (e.g., SST), and aerosol concentration for some rapidly intensifying and weakening TCs using data from the World Wide Lightning Location Network. For example, the rapid intensification of Hurricane Earl (2010) was led by an outbreak of CG lightning after it moved over areas of warmer SST and greater aerosol concentration. There are distinct differences between the distributions of N40 (simulated number concentration of aerosols with diameters larger than 40 nm from Geos-Chem) for samples over ocean and during landfall.

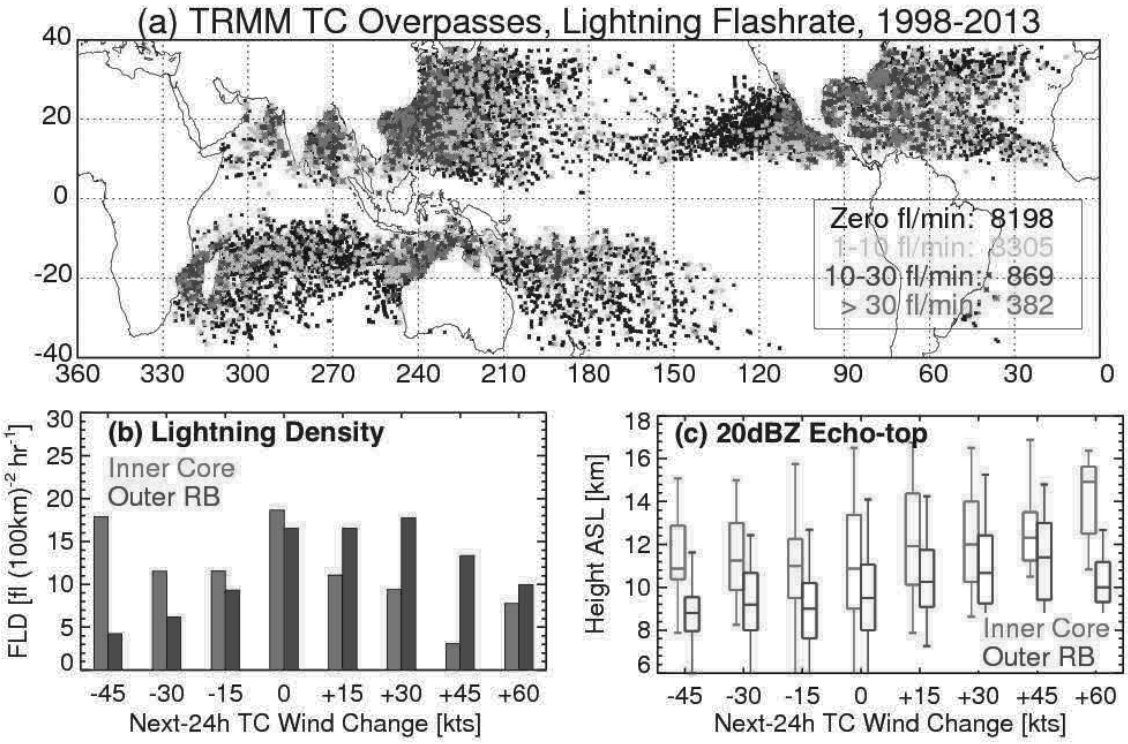

Fig. 1. (a) Geological distribution of TRMM passes over TCs categorized by lightning flash rate. Lightning activity and convective depth 24 h prior to TC intensity change: (b) mean lightning flash density, and (c) 20 dBZ echo-top height. All red and blue bars represent inner core and outer rainband convection, respectively.

RESEARCH ACTIVITY BY INSTITUTIONS

Duke University, Electrical and Computer Engineering Department, Durham, NC USA

Our group continues a recent focus on terrestrial gamma ray flashes (TGFs) in addition to contributing our data and analysis to work led by other research groups. Following our recent work on energetic in-cloud pulses (EIPs) [Lyu et al., GRL, 2015], we have begun to explore the possible relationship between EIPs and TGFs. This work is ongoing and while we have some preliminary conclusions, it is too soon to share details at this point.

We have one published paper led by our group to report. McTague et al. [JGR, 2015] combined NLDN data, ground-based magnetic field data, and Fermi-GBM gamma ray count data in a search for possible nearby, observationally dim TGFs with too few counts to statistically identify with gamma ray data alone. It should be mentioned that our search focused on short horizontal range TGFs (<400 km) to exclude events that are weak only because of horizontal propagation distance. Using NLDN and magnetic field data to identify short (200 microsecond) search windows for Fermi data, we independently found 6 previously-known TGFs. These detections show that the basic approach is capable of finding TGFs with no explicit lower threshold on the number of photons or counts. However, we found no evidence for any TGF counts beyond those from these bright, previously known TGFs. This came as a surprise to us, as we expected to find at least a few lower fluence TGFs given our ability to find higher fluence TGFs. The lack of counts from dim TGFs is statistically inconsistent with a power law distribution of TGF fluence that extends to sub-Fermi threshold TGFs. This indicates that there may be a lower limit to the intrinsic brightness of TGFs, and that there may be lower limit to the altitude at which TGFs occur. More work in this area to bolster the statistical significance of the results is clearly needed.

Indian Institute of Tropical Meteorology, Pune, India

Madhuri N. Kulkarni, mnkulk@tropmet.res.in; mnkulk2005@gmail.com
Devendraa Siingh, devendraasiingh@tropmet.res.in

Application of the model calculated atmospheric electrical columnar resistance to identify the type of El Niño and La Niña events

Atmospheric electrical columnar resistance (R_c) has been calculated using the aerosol optical depths derived from the satellite aerosol measurements and the model (MERRA) derived planetary boundary layer heights. Both the data sets are freely available (courtesy, NASA, USA). The R_c varies with the number concentration of aerosols and their vertical distribution on account of vertical convection. Global circulations are changed during atmospheric events such as ENSO (El Niño Southern Oscillations) or IOD (Indian Ocean Dipole) which change centers of convection and the source regions of aerosols thereby affecting the R_c. Further, changes in circulation are associated with the heat variability. So, we have proposed a new Atmospheric Electrical Index (AEI) which is constructed using the difference in R_c between Tahiti (17.5°S, 150°W) and Darwin (12.5°S, 130°E). We have

found that the average AEI during the Eastern Pacific (EP) ENSO is positive and that during the Central Pacific (CP) ENSO is negative. Number of monthly positive (negative) AEI is greater than that of negative (positive) AEI during the EP (CP) event. 13-month running mean of the AEI has been used to identify the EP and CP events (Figure 1). The intensity of the event can be deduced using the standardized AEI on the time scale of the event. It has also been found that the intensity of La Niña is associated with its duration which is not in the case of El Niño. We find from our correlation results of the AEI and heat variability ENSO modoki being one of the factors responsible for the warming trend slowdown which may be attributed to the mixed (absorbing as well as reflecting-scattering) aerosols during ENSO modoki.

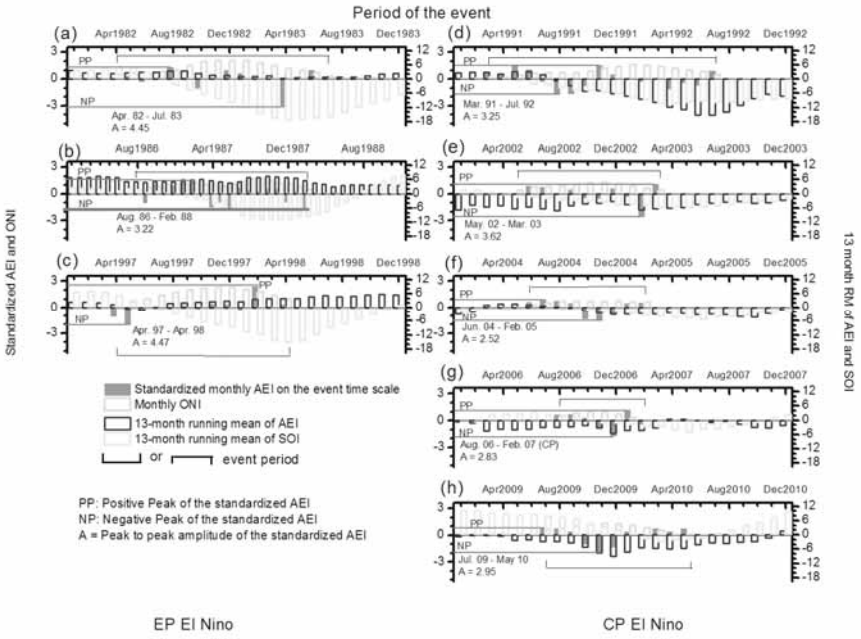

Fig. 1 Identification of the EP and CP ENSO using the Atmospheric Electrical Index (AEI). Figure shows variation of 13-month running mean of the SOI and AEI from January of the starting year to December of the ending year for El Niño, the standardized AEI and the Oceanic Niño Index (ONI) during the event.

Institute of Environmental Research, National Observatory of Athens, Greece)

Lagouvardos Kostas, Kotroni Vassiliki, Karagiannidis Athanassios and Giannaros Theodore
E-mail: lagouvar@noa.gr

In the frame of a national project aiming at the support of Excellency in research, the National Observatory of Athens (NOA hereafter) was granted the project TALOS (Thunderstorm And Lightning Observing and forecasting System). The project, accomplished at the end of 2015 had the following main objectives:

a) Provide a detailed lightning climatology over the Mediterranean area, based on the data provided by the ZEUS lightning detection network, operated by NOA since 2005.

b) Investigate the possible relation of lightning with aerosol load in the atmosphere.
c) Provide a nowcasting tool of lighting activity (1 hour lead time), based on real-time METEOSAT imagery and ZEUS data that is operating in an area covering Greece and surrounding countries.
d) Provide a forecasting toll of lightning activity for Europe and Greece, based on the state-of-the-art WRF model.

The main results of the project can be found in the numerous publications listed at the end of this text. Moreover, an endeavor was accomplished to provide TALOS outputs to the general public. For that purpose, the web page www.thunderstorm24.com was developed, providing the following information:

a) Daily maps of lightning activity over the Mediterranean area since 2005.
b) Maps of current lightning activity over Europe, with zoom facilities etc., updated every 15 min.
c) Convective rainfall rate as deduced by METEOSAT imagery.
d) Lightning forecast maps for the next three days, provided by WRF model.
e) News concerning lightning, useful information on lightning as well as protective measures.

The following two Figures provide snapshots from the web page.

Relevant recent publications

1. Lagouvardos, K., V. Kotroni, E. Defer and O. Bousquet, 2013: Study of a heavy precipitation event over southern France, in the frame of HYMEX project: Observational analysis and model results using assimilation of lightning. Atmospheric Research, *Volume 134*, *1 December 2013*, *Pages 45-55*.

2. Petrova S., R. Mitzeva and V. Kotroni, 2014: Summer-time lightning activity and its relation with precipitation: diurnal variation over Maritime, Coastal and Continental Areas, Atmospheric Research. Atmospheric Research, 135–136, 388–396.

3. Giannaros, Th, V. Kotroni, K. Lagouvardos, 2015: Predicting Lightning Activity in Greece with the Weather Research and Forecasting (WRF) Model. Atmospheric Research, 156, 1-13.

4. Defer, E., Pinty, J.-P., Coquillat, S., Martin, J.-M., Prieur, S., Soula, S., Richard, E., Rison, W., Krehbiel, P., Thomas, R., Rodeheffer, D., Vergeiner, C., Malaterre, F., Pedeboy, S., Schulz, W., Farges, T., Gallin, L.-J., Ortéga, P., Ribaud, J.-F., Anderson, G., Betz, H.-D., Meneux, B., Kotroni, V., Lagouvardos, K., Roos, S., Ducrocq, V., Roussot, O., Labatut, L., and Molinié, G., 2015: An overview of the lightning and atmospheric electricity observations collected in southern France during the HYdrological cycle in Mediterranean EXperiment (HyMeX), Special Observation Period 1, Atmos. Meas. Tech., 8, 649-669, doi:10.5194/amt-8-649-2015.

5. Galanaki E., V. Kotroni, K. Lagouvardos, and A. Argiriou, 2015: A ten-year analysis of lightning activity over the Eastern Mediterranean. Atmospheric Research, 166, 213-222.

6. Karagiannidis A., K. Lagouvardos, V. Kotroni, 2016: The use of lightning data and Meteosat Infrared imagery for the nowcasting of lightning activity. Atmospheric Research, 168 (2016) 57–69, doi: 10.1016/j.atmosres.2015.08.011.

7. Giannaros, Th, V. Kotroni, K. Lagouvardos, 2016: WRF-LTNGDA: A Lightning Data Assimilation Technique Implemented In The Wrf Model For Improving Precipitation Prediction. Environmental Modelling & Software, 76, 54-68.

8. Proestakis, E., S. Kazadzis, K. Lagouvardos, V. Kotroni, A. Kazantzidis, 2016: Lightning activity and aerosols in the Mediterranean region. Atmospheric Research, 170, 66-75.

9. Kotroni V. and K. Lagouvardos, 2016: Lightning in the Mediterranean and its relation with sea-surface temperature. Environmental Research Letters, 11, 034006.
10. Karagiannidis A., K. Lagouvardos, V. Kotroni, and N. Mazarakis, 2016: Investigation of single-cell thunderstorms lightning activity using METEOSAT rapid scan infrared imagery. International Journal of Remote Sensing (in press).
11. Galanaki E, E. Flaounas, V. Kotroni, K. Lagouvardos and A. Argiriou, 2016: Lightning activity in the Mediterranean: Quantification of cyclones contribution and relation to their intensity. Atmospheric Science Letters (under review).
12. Proestakis, E., S. Kazadzis, K. Lagouvardos, V. Kotroni, V. Amiridis, E. Marinou, C. Price and A. Kazantzidis, 2016: Aerosols and lightning activity: the effect of vertical profile and aerosol type. Atmospheric Research (under review).
13. Giannaros Th., K. Lagouvardos, and V. Kotroni, 2016: Performance evaluation of an operational lightning forecasting system in Europe. Natural Hazards (under review).

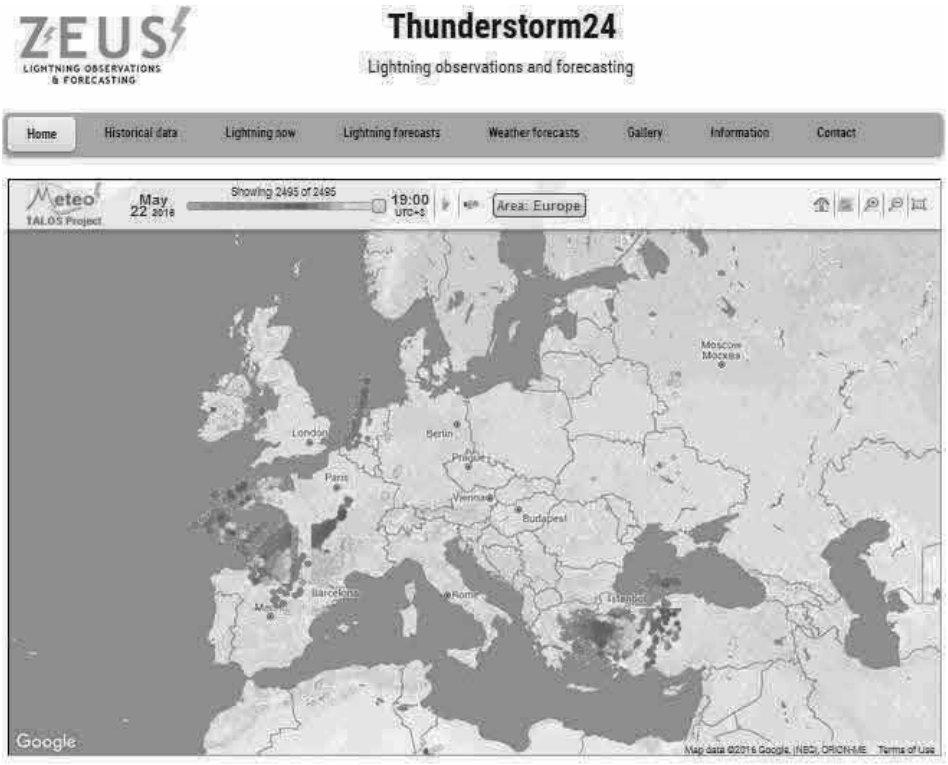

Fig. 1 Map of lightning activity, as detected by NOA ZEUS system on 22rd May 2016.

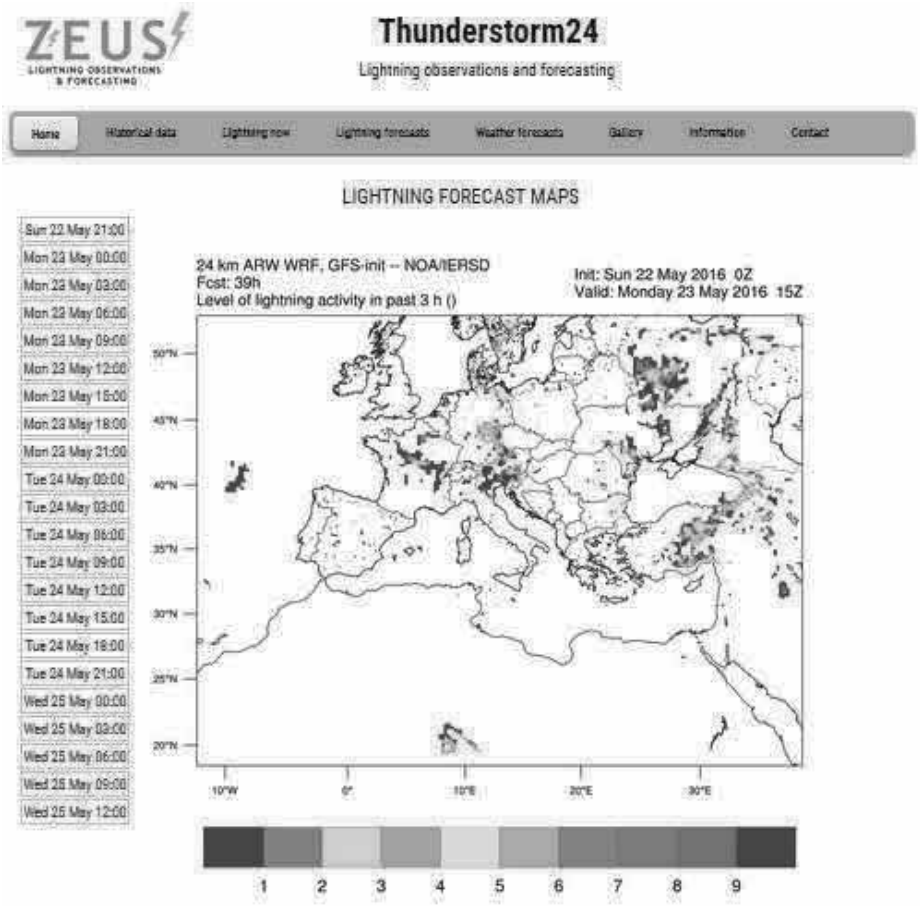

Fig. 2: Example of forecast map on lightning activity based on WRF model.

Ioffe Institute, St. Petersburg, Russia

Mikhail L. Shmatov

TGF and ball lightning studies

The author has proposed a model for the initial acceleration of electrons of terrestrial gamma-ray flashes (TGFs) with a hard spectrum, according to which this acceleration occurs on screening of the strong electric field near the lateral surface of a new conducting region arising at the formation of a new step of a negative leader of lightning after the contact of a head of a positive volume leader with the channel of the main leader (M.L. Shmatov 2015a, New model of initial acceleration of electrons of terrestrial gamma-ray flashes with a hard spectrum, Physics Letters A, 379, 1358–1360). The number of electrons undergoing such acceleration during the formation of one leader step can be of the order of 10^{17}.

The author has also proposed a ball lightning model according to which the motion of the electrons in the ball lightning core is the superposition of oscillatory motion and thermal motion in directions perpendicular to whose of oscillations (M.L. Shmatov 2015b, Ball lightning with the nonrelativistic electrons of the core, J. Plasma Phys. 81, 905810406). This model results from the development of the model taking into

account only the oscillatory motion of the electrons (M.L. Shmatov 2003, New model and estimation of the danger of ball lightning, J. Plasma Phys. 69, 507–527). Its main advantage is related to the improved analysis of the recombination processes. When the ball lightning core is spherical, the oscillatory motion is radial and the main loss of ball lightning energy is due to bremsstrahlung. At an atmospheric pressure of about 10^5 Pa, the lifetime τ_c of the ball lightning core is of the order of 1 s when the initial value $\varepsilon_{osc}^{\max 1}$ of the maximum kinetic energy, corresponding to oscillatory motion, is several tens of keV. An increase in $\varepsilon_{osc}^{\max 1}$ increases τ_c.

In the ball lightning core, ions of N and O are almost totally ionized, while ions of Ar have the typical ionization stage of 16 to 18. The stability of ball lightning core is provided by the oscillation of its particles and the atmospheric pressure that compensates for the outward forces arising due to the three-dimensional geometry of the oscillations and random motion of the particles. The core is isolated from the atmosphere by the depleted region. The maximum volume density of ball lightning energy is of the order of 1 kJ/cm^3.

Ball lightning arises due to the formation of converging flux of runaway electrons. A model for the initial acceleration of such electrons has been presented, according to which this acceleration occurs on screening of the strong electric field of the positive charge injected into the atmosphere (M.L. Shmatov 2015c, Possible scenarios for the initial acceleration of electrons of the core of ball lightning, J. Plasma Phys. 81, 905810607). This model is similar to that proposed to explain the initial acceleration of electrons of TGFs with a hard spectrum (Shmatov 2015a). Several scenarios for the injection of the positive charge, the factors favorable for the formation of ball lightning and possible experiments on the formation of ball lightning are considered. The geometries of two possible experiments are shown in Fig. 1. For the geometry shown in Fig. 1a, the formation of ball lightning is probably possible only when ordinary cloud-to-ground lightning striking an ungrounded elongated conductor is positive. This geometry corresponds to a number of reports about the observed formation of ball lightning and to the available information about the circumstances of the death of Prof. G.-W. Richman (see e.g. S. Singer 1971, The Nature of Ball Lightning, Plenum; Stakhanov 1996, About the Physical Nature of Ball Lightning, 3rd ed., Nauchnyi Mir (in Russian). For the geometry shown in Fig. 1b, the formation of ball lightning is possible at any sign of ordinary cloud-to-ground lightning (when this sign is negative, the injection of the positive charge into the atmosphere will occur at the return stroke). This geometry corresponds to the experiment performed by A.A. Marvin (Stakhanov 1996, p. 148, report No. 117; see also Shmatov 2015c).

The model under consideration corresponds to the assumptions about the high radiation hazard of some ball lightning (see e.g. Stakhanov 1996, p. 17; Shmatov 2003, 2015c and bibliography therein). Therefore, in experiments on the formation of ball lightning, safety measures related to the radiation hazard should be taken. Note that the first assumption about the emission of high-energy photons by ball lightning was published in 1966 (P. J. Klass 1966, Many UFOs are identified as plasmas, Aviation Week & Space Technology, 85 (14), 54–73).

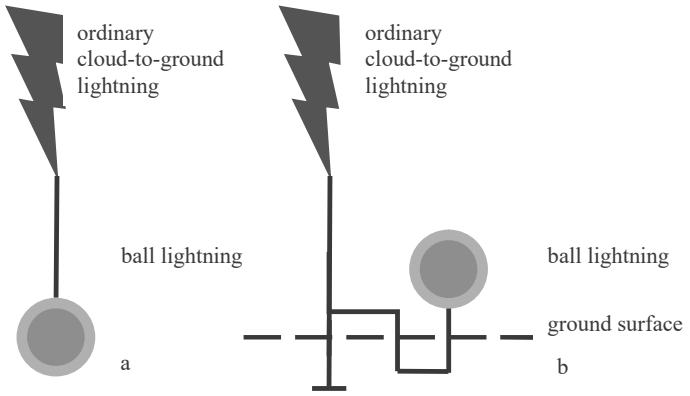

Fig.1 The geometries of some possible experiments on the formation of ball lightning with the use of ordinary cloud-to-ground lightning. Thick solid lines denote conductors. Isolation of the underground part of one of the conductors in Fig. 1b is not shown.

Israel Atmospheric Electricity Group (Tel Aviv University and Interdisciplinary Center)

Profs. **Colin Price** (Tel Aviv University) and **Yoav Yair** (Interdisciplinary Center, Herzliya) continue with their joint research in Atmospheric Electricity.

Our fair weather electrical studies have expanded to studying dust storm electrification (MSc student **Shai Katz**) where we have measured fields of 8kv/m at the surface on days of heavy dust in the Negev desert. PhD student **Roy Yaniv** has analysed the diurnal cycle of the potential gradient in Israel, showing a strong local morning aerosol effect (Yaniv et al., 2016), as well as the "Aschtauch" mountain effect on the Ez observations. In addition, we continue to study solar impacts on the fair weather fields and current density. We have also continued our balloon launches from Mitzpe Ramon to study the cosmic ray ionization above Israel. In the coming months we plan to use drones to attempt measurements in the boundary layer during fair-weather and dusty conditions.

Graduate students **Gil Averbuch** and **David Applbaum** are working on problems related to infrasound, using the two infrasound stations found in Israel. We detect infrasound signals from sprites, thunderstorms, ocean swells, and a very clear signal from Mt. Etna eruptions in Sicily.

Graduate student **Gal Elhalel** continues her laboratory studies on the impact of the Schumann resonances on biological systems. We have been working with heart muscles from mice, and have detected very interesting, reversible, impacts of weak ELF fields on the spontaneous contractions of heart muscle. We hope to write up the results soon.

PhD student **Israel Silber** is working in the field of VLF narrowband observations. We have recently published an interesting paper on the semi-annual cycle detected in narrowband VLF signals (Silber et al., 2016). In addition, we have also detecting gravity waves and infrasound signal in the narrowband signals measured in Israel. We think these waves are due to thunderstorms in the region generating gravity waves that propagate aloft to the

D-region. Israel has just finished his PhD and will soon be starting a postdoc position at Penn State in cloud physics.

Work with former student Dr. **Yuval Reuveni** (now at Ariel University) has been directed toward the possible detection of terrestrial ground enhancements (TGEs) below or in the vicinity of thunderstorms. We have installed two gamma-ray detectors on Mt. Hermon to study links between radon emissions and the potential gradient. Our initial results show enhanced gamma-rays detected during thunderstorms lasting for up to 30 minutes at a time.

Finally, MSc students **Shay Frankel** and **Maayan Harel** continue to work with the WWLLN data to study thunderstorms in hurricanes (SF) and over Africa (MH). We have shown that information about the number and size of thunderstorm clusters in hurricanes can help improve the 24-48 hour of hurricane intensity. Maayan is working on understanding the link between climate parameters over Africa and the number and size of thunderstorm clusters. This study will help develop parameterizations for modeling the impact of climate change in thunderstorm cells in Africa. **Laura Ihrlich** from Germany spent a 4-month internship with our group to develop a simple nowcasting scheme over Africa using WWLLN data. We have shown that the WWLLN data may be a very useful dataset for nowcasting in regions of the world where no other meteorological data is available for end users and stakeholders.

Laboratoire d'Aérologie, Université de Toulouse, (Toulouse, France)

The lightning climatology in a 2750 km × 2750 km area of the Congo Basin (10°E - 35°E; 15°S - 10°N), including several countries of Central Africa, has been analysed in detail (Soula et al., 2016). The study is based on data from the World Wide Lightning Location Network (WWLLN), for the period from 2005 to 2013. A comparison of these data with Lightning Imaging Sensor (LIS) data for the same period shows the relative detection efficiency of the WWLLN (DE) in the region increases from ~ 2 % during the first four years to ~ 6 % in 2013. The trend is the same as in other parts of the world. However, the increase of DE is not uniform over the whole region and by comparing with ocean regions, it is lower and it increases less rapidly. The annual cycle of lightning activity exhibits a period of high activity between October and March, during which about 10 % of the total lightning flashes are produced each month, and a period of low activity from June to August with about 4.5 % of the total flashes produced each month. This seasonal variation is associated with the ITCZ migration but not exactly symmetrical on both sides of the equator. The zonal distribution of the lightning flashes exhibits a maximum between 1°S and 2°S and about 56 % of the flashes are located south of the equator in the 10°S – 10°N interval. The diurnal evolution of the flash rate has a maximum between 1400 and 1700 UTC, according to the reference year. The annual flash density and number of stormy days show a sharp maximum localized in the eastern part of Democratic Republic of Congo (DRC), west of Kivu Lake, regardless of the reference year and the period of the year. These maxima reach 12.86 fl km^{-2} and

189 days in 2013, respectively, and correspond to a very active region located at the rear of the Virunga mountain range at altitudes that exceed 3000 meters. The presence of these mountains plays a role in the thunderstorm development along the year. The estimation of this local maximum of the lightning density by taking into account the DE (5.9 % in 2013), leads to more than 200 fl km^{-2} y^{-1} at a resolution of 0.1° × 0.1°, which is consistent with the values issued from the global climatology. Furthermore, the maximum number of flashes per stormy day is located in the same region, which means the thunderstorms are there, more numerous, more intense, more stationary, or all three at once.

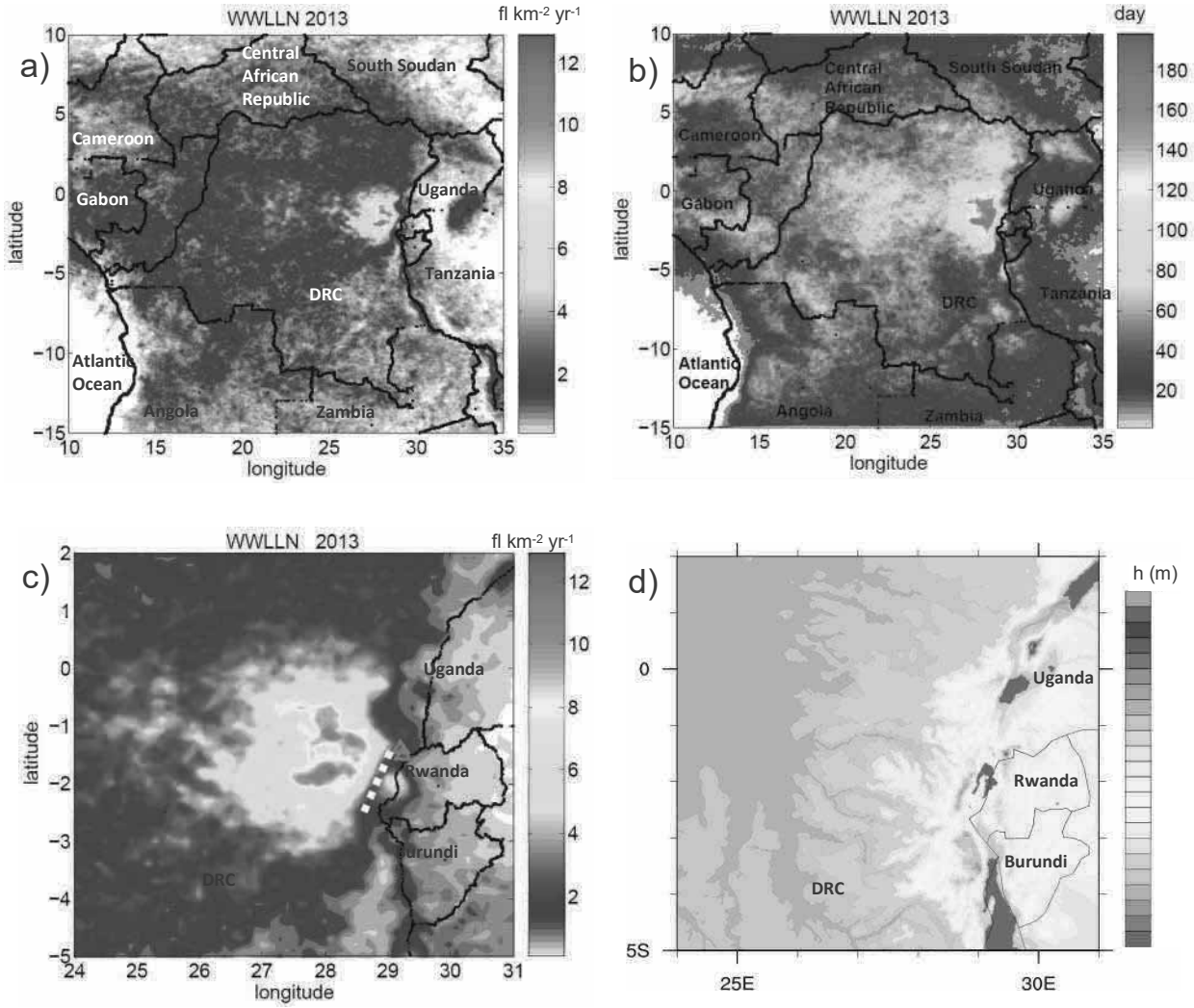

Fig. 1 Lightning density detected by WWLLN in 2013 with a 5.9% efficiency (resolution 0.1°) for the entire study area (a), and the maximum area of activity (c) where the white dotted line is the mountain range of Mitumba and two red triangles two active volcanoes. (b) Number of days of thunderstorms for 2013 (same resolution). (d) orography in the area of maximum activity.

Laboratory of Lightning Physics and Protection Engineering (LiP&P), Chinese Academy of Meteorological Sciences (CAMS), Beijing, China

High-speed video observations of a natural negative stepped leader at clos distance

High-speed video observations of a natural downward negative lightning flash that occurred at a close distance of 350 m were presented. The stepped leader of this flash was imaged by three high-speed video cameras operating at framing rates of 1,000, 10,000 and 50,000 frames per second, respectively. Synchronized electromagnetic field measurements for the negative stepped leader were also obtained using the flat-plate fast antenna, the flat-plate slow antenna, and the crossed-loop magnetic field antenna. Based on those optical and electromagnetic observations, three main conclusions were achieved:

(1) First, several detailed features of the stepping process in leader branches were identified in the high-speed video records. A total of 23 luminous segments, commonly attributed to space stems/leaders, were captured. Their two-dimensional lengths varied from 1 to 13 m, with a mean of 5 m. The distances between the luminous segments and the existing leader channels ranged from 1 to 8 m, with a mean value of 4 m. Weakly luminous filamentary structures, which we interpreted as corona streamers, were observed emanating from the leader tip. The stepped leader branches extended downward with speeds ranging from 4.1×10^5 to 14.6×10^5 m s^{-1}.

(2) Second, nine pronounced field pulses which we attributed to individual leader steps were observed in electromagnetic field records. The time intervals between the step pulses ranged from 13.9 to 23.9 μs, with a mean value of 17.4 μs. Further, for the first time, smaller pulses were observed between the pronounced step pulses in the magnetic field derivative records. The smaller pulses may relate to impulsive processes occurring between steps. Time intervals between the smaller pulses (indicative of intermittent processes between steps) ranged from 0.9 to 5.5 μs, with a mean of 2.2 μs and a standard deviation of 0.82 μs.

(3) Finally, based on our observations, we proposed a generalized leader step formation process in natural negative leader and three possible space stem/leader development scenarios. The leader step-formation process is decomposed into five stages, and at the last stage, some space stems/leaders may still exist near the lateral surface of the newly extended leader channel. For this kind of space stems/leaders, three possible development scenarios (the development of the existing channel is ignored) were inferred: A, the space stem/leader fails to make connection to the leader channel; B, the space stem/leader connects to the existing leader channel, but may die off and be followed, tens of microseconds later, by a low luminosity streamer; C, the space stem/leader connects to the existing channel and launches an upward-propagating luminosity wave. Due to limited time resolution, the scenarios are somewhat speculative and, hence, further research is required (Fig. 1).

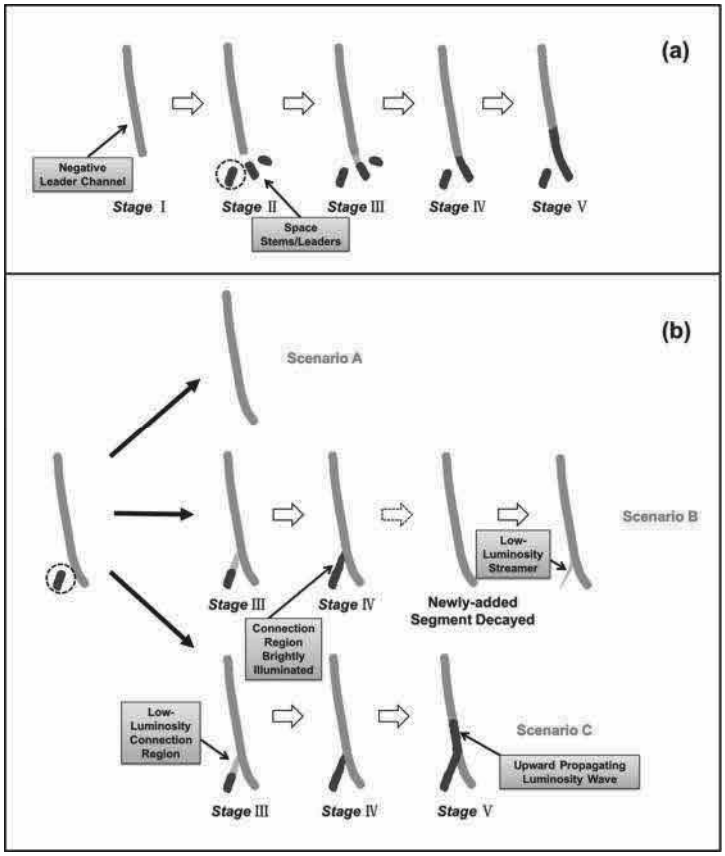

Fig. 1 (a) Sketches of leader step formation process and (b) three possible space stem/leader development scenarios (A, B, and C).

Two basic leader connection scenarios observed in negative lightning attachment process

As the downward leader (DL) and the upward connecting leader (UCL) approach each other, it is generally thought that the DL's tip and the UCL's tip will come in contact with each other. However, Lu et al. (GRL, 2013) presented a negative lightning flash in which the attachment process exhibited an unexpected behavior. The connection of the DL's tip to the lateral surface of the UCL was first reported. Are there any other scenarios leading to the contact of the DL and the UCL?

High-speed video images of 24 downward negative lightning flashes terminating on tall structures in Guangzhou are selected to analyze the connecting behavior of the downward and upward leaders during the attachment process preceding the first return stroke. Three types of leader connecting behavior have been observed: Type I, the tip of DL to the tip of UCL, which accounts for 42% of all the events (10/24); Type II, the DL's tip to the lateral surface of UCL, which accounts for 50% (12/24); and Type III, the combination of Types I and II, which accounts for 8% (2/24). For the two cases of Type III behavior, each case had two junction points (one with Type I and the other with Type II behavior) between the downward and upward leaders. Therefore, Types I and II can be viewed as the two basic types of the leader connecting behavior during the attachment process in negative lightning. No attachment process exhibited the connection of the UCL's tip to the lateral surface of DL. The presence of multiple DL branches and their integrated effect on the development of positive UCL/UCLs are likely to be the main reasons for the Type II behavior (Fig. 2 and Fig. 3).

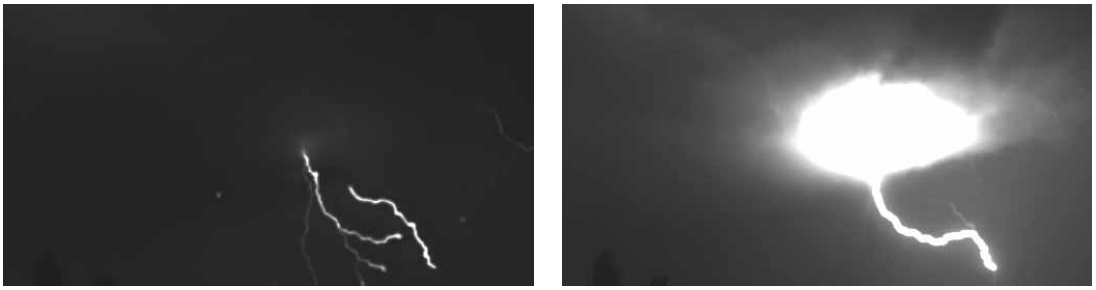

(a) (b)

Fig. 2 An example of Type II leader connecting behavior. Two frames of the high-speed images of a flash captured by a high-speed camera with a sampling rate of 50,000 fps. (a) the last frame preceding the first return stroke, (b) the ninth frame after the first return stroke.

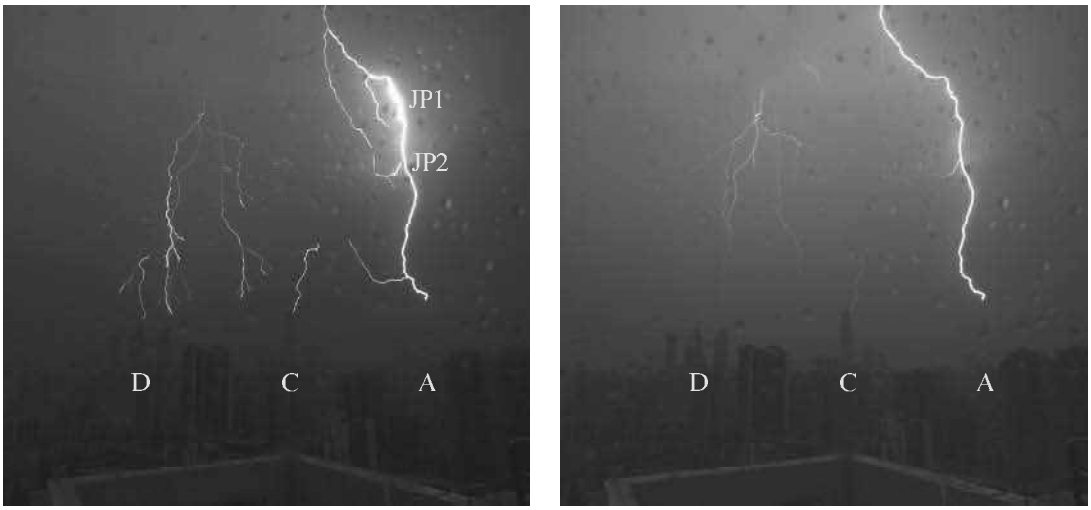

(a) -0.10~0.00 ms (b) 0.30~0.40 ms

Fig. 3 An example of combination leader connecting behavior (Type I + Type II). Two frames of the high-speed images of a flash captured by a high-speed camera with a sampling rate of 10,000 fps. In (a), the first connection occurred at JP1 and the second connection did not occur yet (note a small gap near the bright channel). Most pixels in the frame subsequent to (a), which is not shown here, are saturated. The return stroke channel in (b), which is the fourth frame after the first return stroke, shows that there exists a second connection (at JP2) between a branch of the DL and the lateral surface of the UCL.

Simultaneous optical and electrical observations of "chaotic" leaders preceding subsequent return strokes

Based on the synchronous optical-electrical data of natural cloud-to-ground flashes observed from Guangdong Comprehensive Observation Experiment on Lightning Discharge (GCOELD), "chaotic" leaders have been investigated. 44% of subsequent return strokes are preceded by "chaotic" leaders which are characterized by chaotic pulses during the subsequent leader process. Almost all of "chaotic" leaders are accompanied by chaotic E-change and obvious optical radiation. Two types of "chaotic" leaders (type I and type II) with the percentages of 65% and 35% have been identified. Type I exhibits continuously chaotic fast E-change pulses prior to subsequent return stroke, however, type II begins

with large chaotic pulses in the fast E-change waveform and then some weak pulses occur in the following waveform preceding subsequent return stroke. The preceding inter-stroke intervals for type I and type II are 54.13 ms and 72.51 ms, respectively. The amplitude ratios of chaotic pulses to the following return stroke for the fast E-change signals of type I and type II are 0.17 and 0.41, and the corresponding ratios for the optical signals of type I and type II are 0.25 and 0.38, respectively. The durations of chaotic pulses for type I and II are 559.9 μs and 414.2 μs. Compared to type I, type II owns the characteristics with larger amplitude ratios of chaotic pulses to the following return stroke, which indicates that type II is associated with a stronger discharge process. It is possible that the characteristics of "chaotic" leaders are partly related to preceding inter-stroke intervals. Two cases with synchronous high-speed video images further depict the two "chaotic" leaders. The leader of type I propagates along one channel branch of previous return stroke to reach ground and the propagation channel is branched. As a comparison, the leader of type II propagates along one prior channel branch at first and then the channel dims accompanied by strong luminosity (Fig. 4 and Fig. 5).

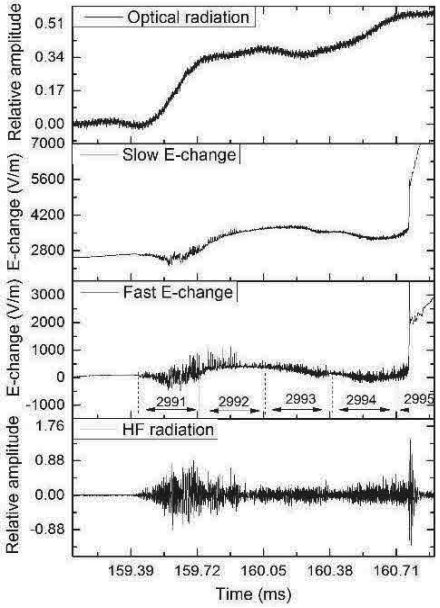

Fig.4 E-change, optical radiation and HF radiation waveforms of type II

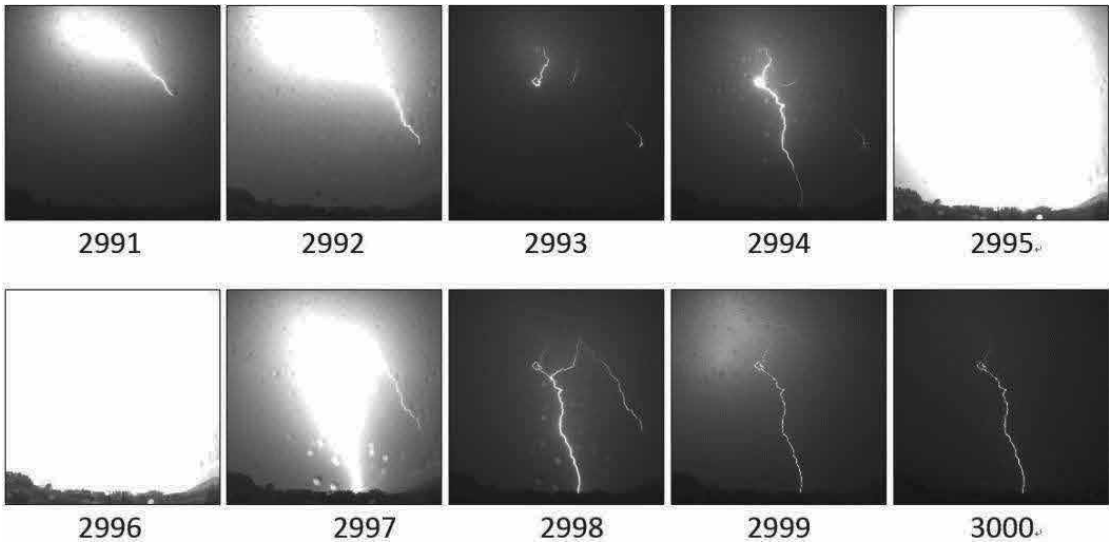

Fig.5 Images of the third RS and the corresponding leader

Impact of the Vertical Velocity Field on Charging Processes and Charge Separation in a Simulated Thunderstorm

A 3D charging–discharging cloud resolution model was used to investigate the impact of the vertical velocity field on the charging processes and the formation of charge structure in a strong thunderstorm. The distribution and evolution of ice particle content and charges on ice particles were analyzed in different vertical velocity fields. The results show that the ice particles in the vertical velocity range from 1 to 5 m s^{-1} obtained the most charge through charging processes during the lifetime of the thunderstorm. The magnitude of the charges could reach 10^{14} nC. Before the beginning of lightning activity, the charges produced in updraft region 2 (updraft speed ≥ 13 m/s) and updraft region 1 (updraft speed between 5 and 13 m/s) were relatively significant. The magnitudes of charge reached 10^{13} nC, which clearly impacted upon the early lightning activity. The vertical velocity conditions in the quasi-steady region (updraft speed between −1 and 1 m s^{-1}) were the most conducive for charge separation on ice particles of different scale. Accordingly, a net charge structure always appeared in the quasi-steady and adjacent regions. Based on the results, a conceptual model of ice particle charging, charge separation and charge structure formation in the flow field was constructed. The model helps to explain observations of the "lightning hole" phenomenon (Fig. 6).

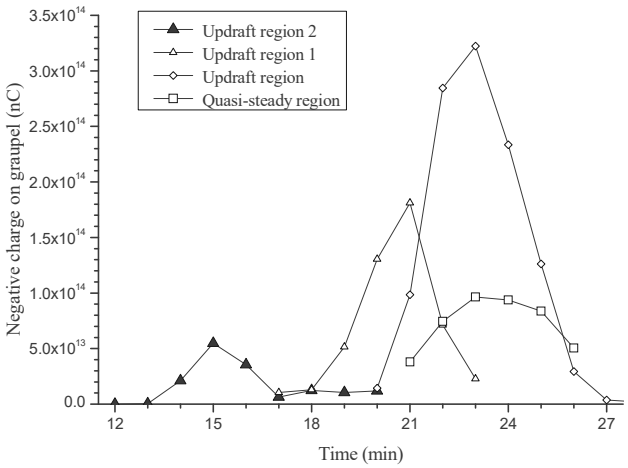

Fig. 6 Evolution of negative charge on graupel due to the charging processes in different vertical velocity ranges.

Impact of Updraft on Neutralized Charge Rate by Lightning in Thunderstorms: A Simulation Case Study

The rate of neutralized charge by lightning (RNCL) is an important parameter indicating the intensity of lightning activity. The charging rate (CR) in a thunderstorm, the changing rate of the total amount of one kind of polarity (e.g., negative) charge (CROP) in a thunderstorm, and the outflow rate of charge on precipitation (ORCP), are proposed as key factors impacting RNCL, based on the principle of conservation of one kind of polarity charge in a thunderstorm. To comprehensively understand the impact of updraft on RNCL, analysis is carried out that focuses on the impact of updraft on CR and CROP. The results show that updraft both promotes and inhibits RNCL at the same time: (1) Updraft always has a positive influence on CR. The correlation coefficient between the updraft volume and CR can reach 0.96. Strengthening of the updraft advances the strengthening of RNCL through this positive influence. (2) Also, strengthening of the updraft promotes the reinforcement of CROP. The correlation coefficient between the updraft volume and CROP is high (about 0.9), but this promotion restrains the strengthening of RNCL because the strengthening of CROP will, most of the time, inhibit the increasing of RNCL. Additionally, the increasing of ORCP will depress the strengthening of RNCL. In terms of magnitude, the peak of ORCP is equal to the peak of CR. Because the main precipitation always appears after the lightning activity finishes, the depression effect of ORCP on RNCL can be ignored during the lightning activity period (Fig. 7).

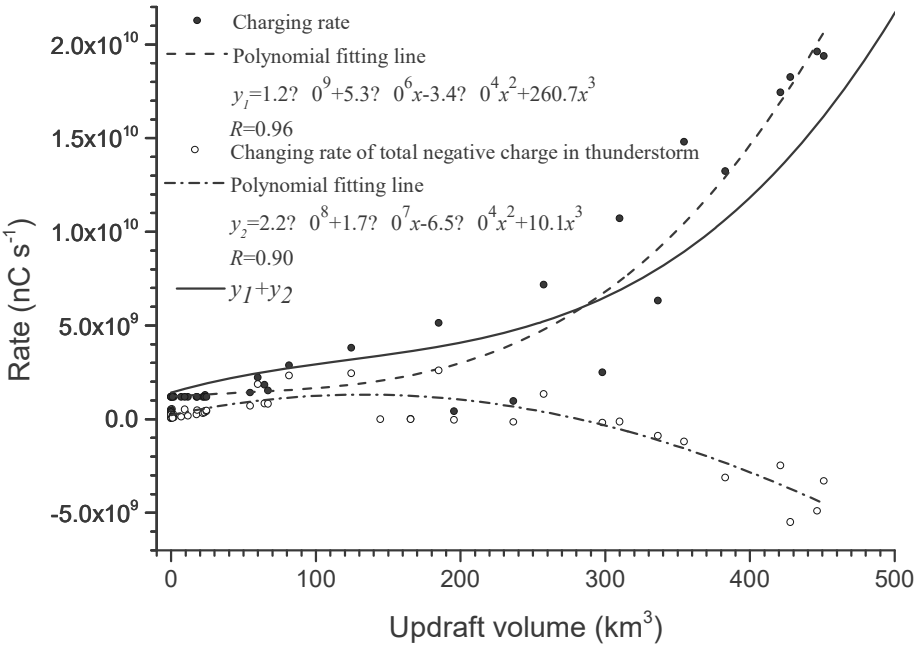

Fig. 7 Combined effect of the charging rate and changing rate of total negative charge in the thunderstorm.

Characteristics of flash initiations in a supercell cluster with tornadoes

Flash initiations within a supercell cluster during 10–11 May 2010 in Oklahoma were investigated based on observations from the Oklahoma Lightning Mapping Array and the Norman, Oklahoma, polarimetric radar (KOUN). The flash initiations at positions dominated by graupel, dry snow, small hail and crystals accounted for 44.3%, 44.1%, 8.0% and 3.0% of the total flashes, respectively. During the tornadic stage of the southern supercell in the cluster, flash initiations associated with graupel occupied the main body, the right flank and the forward flank of the supercell, while those associated with dry snow dominated the outskirts of the adjacent forward anvil, right anvil and rear anvil. The flash initiations associated with small hail were concentrated around the main updraft, particularly toward its front side. Highly dense flash initiations were located in the regions overlying the differential reflectivity (Z_{DR}) arc and right anvil. The average initial height of the flashes decreased gradually from the rear to the front and from the right to the left flanks, while the height range over which initiations occurred reached a maximum at the front of the updraft. The flashes that were initiated in the adjacent forward anvils were largest on average, followed by those in the regions ahead of the updraft and near the Z_{DR} arc. This study supports the concept of charge pockets and further deduces that the pockets in the right anvil are the most abundant and compact due to the frequent flash initiations, small-sized flashes and thin layers including flash initiations.

Climatological comparison of small- and large-current cloud-to-ground lightning flashes over Southern China

The first climatological comparison of small-current cloud-to-ground (SCCG; peak current ≤50 kA) and large-current cloud-to-ground (LCCG; peak current >50kA, >75 kA, and >100 kA) lightning flashes is presented for southern China. The LCCG lightning exhibits an apparent

preference to occur over the sea. The percentage of positive LCCG lightning during the nonrainy season was more than twice that during the rainy season, while the percentage of positive SCCG lightning showed small seasonal differences. Positive cloud-to-ground (PCG) lightning was more likely to feature a large peak current than was negative cloud-to-ground (NCG) lightning, especially during the nonrainy season and over land. Distinct geographical differences are found between SCCG and LCCG lightning densities and between their own positive and negative discharges. Furthermore, the percentages of positive lightning from LCCG and SCCG lightning exhibit distinctly different geographical and seasonal (rainy and nonrainy season) distributions. The diurnal variations in SCCG and LCCG lightning are clearly different over the sea but similar over land. Diurnal variations in the percentage of positive lightning are functions of the peak current and underlying Earth's surface. In combination with the University of Utah precipitation feature (PF) dataset, it is revealed that thunderstorms with relatively weak convection and large precipitation areas are more likely to produce the LCCG lightning, and the positive LCCG lightning is well correlated with mesoscale convective systems in the spatial distribution during nonrainy season.

Lightning research group of Gifu University (Gifu, Japan)

Daohong Wang, Shintaro Kuroda and Nobuyuki Takagi have analyzed the lightning attachment processes of 19 negative and 2 positive natural CG recorded by using a high speed optical system during the past 5 years at the International Center for Lightning Research and Testing (ICLRT), Camp Blanding, Florida. We have obtained not only their stepped leader speeds and the return stroke speeds near the channel bottoms, but also their return stroke initiation heights. Most of the negative first return strokes exhibited an initiation height of 40 m or so. Return strokes with bigger peak current tend to initiate higher. For one positive first stroke, although its peak current is much larger than all the negative counterparts, its initiation height is smaller than most of the negative ones. The detailed result will be presented in the next ICLP.

Meanwhile, we have continued our observation on lightning that strike on a rotating windmill and its nearby lightning protection tower during last winter season. The recorded data is under analysis. With the data recorded during 2014 winter season, Daohong Wang, Norio Sawamura and Nobuyuki Takagi have analyzed the optical progression characteristics of an upward connecting negative leader and a downward positive dart leader contained in a positive lightning discharge that hit on the blade tip of a windmill. The pulse discharges in the negative leader are found to propagate backward usually with a distance of a few tens of meters. Their propagation speeds tend to be around 1.0×10^8 m/s initially and soon drop to a stable value of about 2.0×10^7 m/s. The downward positive dart leader also exhibited a speed of about 2.0×10^7 m/s, not different from a usual negative dart leader. The plasma formed on the windmill blade tip by the lightning tends to be much brighter than the free space lightning channel. These results will be presented in the next ICLP as well.

From June, Ting Wu, currently a post doctor working for Osaka University, will join our research group as an assistant professor.

MIT Parsons Laboratory (Cambridge, MA, USA)

Earlier documentation on inverted polarity clouds from the STEPS (Severe Thunderstorm Electrification and Precipitation Study) in 2000 in eastern Colorado has been re-examined from a thermodynamics standpoint. The easily accessible surface dew point depression at surface meteorological stations has been used as a reliable measure of cloud base height for storms documented electrically by Fleenor et al. (2009) and by Rust et al. (2005). Single cell storms with a high percentage of ground strokes with single polarity also show distinct differences in cloud base height (and temperature), with the conspicuous inverted polarity (+CG dominant storms) showing exceptionally high cloud bases. The earlier suggestion (Williams et al., 2005) that a wet growth condition might be involved now seems unlikely on the basis of parcel theory calculations involving lifting from cloud base height and comparisons with cloud water content needed for wet growth of rimed ice particles. A high cloud base will guarantee smaller cloud droplet sizes in the charging region regardless of the CCN condition at cloud base height. In laboratory studies, Avila and Pereyra (2000) found a tendency for positive charging of rimed ice with smaller droplet size. This work is one component of an NSF-supported study with Dick Orville (Texas A&M), Danny Rosenfeld (Hebrew University, Israel) and Don MacGorman (NSSL).

Earle Williams attended the WOMEL (World Meeting on Lightning) conference in Cartagena, Colombia in April and presented a paper entitled: "Global Lightning Activity and the Hiatus in Global Warming", collaborative work with Hugh Christian, Dennis Buechler, Anirban Guha and Bob Boldi. Discussion was also held there with atmospheric electricians in Bogota (Horacio Torres, Daniel Aranguren, and Camilo Younes) on the problem of inverted polarity clouds, given the high cloud bases that are frequent in their Andes thunderstorms.

The Grainger Foundation has generously provided private support for Schumann resonance work, by virtue of a matching arrangement with the Geodetic and Geophysical Institute of the Hungarian Academy of Sciences (Erno Pracser and Gabriella Satori) and MIT. The main goal will be the continuation of the inversion of multi-station Schumann resonance background observations for the global lightning activity in absolute units. Two approaches to be pursued are the sensitivity matrix treatment initiated by the late Vadim Mushtak and the Green's function approach developed initially by Madden and Nelson, and revitalized independently by Haiyan Yu at MIT and by Erno Pracser in Hungary. New ELF station observations in Cuba and Mexico (B. Mendoza), Argentina (E. Avila and SR group in Poland), China (H. Yu and X. Zhang), Colorado USA (SR group in Poland), Greece (P. Kostarakis), Greenland (R. Moore), Scotland (C. Beggan), and Spain (S. Toledo-Redondo) are expected to provide a major supplement to the earlier collection of nine stations. Anirban Guha has recently been awarded a Raman Fellowship in India and will return to MIT in the Fall to resume this work.

National Cheng Kung University (Taiwan)

Yen-Jung Wu

The work on the collocation of OH nightglow and elve altitude has experienced an important breakthrough in the past few months. The ISUAL team at the National Cheng Kung University, Taiwan, has undertaken a rigorous calibration on the OH and elve heights in the limb through the use of stars in the image field. Considering the background and the dynamic range of the instrument, this method requires at least two stars brighter than visual magnitude 3 in the image to identify the stars correctly. As many as 10 stars frequently show up in the image and are chosen as reference points for satellite positioning. The referencing stars have been carefully observed about 2000 times over the satellite lifetime from 2004 to 2015. With these calibrated images, the long term drift pertaining to the orbital precession of the Earth has been clearly identified, which causes a 0.1 degree change over a decade. The effect of the oblate spheroidal shape for Earth on elve and OH height estimation is then taken into account after star calibration. The Earth radius is 6378 km at the equator in contrast with 6356 km at the pole. Though the difference in radius is less than 30 km, this impacts significantly the height estimation of targets of interest at the limb in the images recorded from space. In the revised data set with corrected heights, the semiannual variation of elve height in the lower range of latitude is revealed (Fig. 1). The semiannual pattern is the featured signal of the OH variation from the long term observation by SCIAMACHY, another satellite designed specifically for high precision observations on OH airglow. This is not only the natural result of the collocation of the OH height and elves, but also a new finding on the spatial variation of elves.

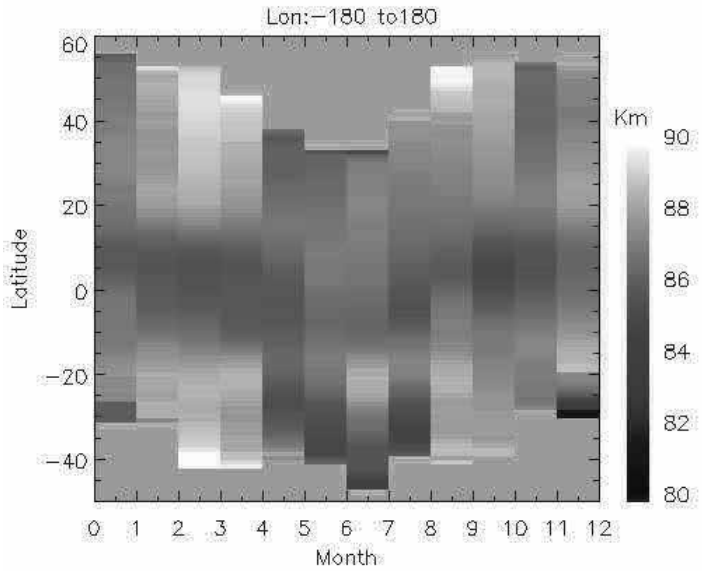

Fig. 1 Altitude variation of OH nightglow observed by ISUAL.The semiannual pattern at the lower range of latitude is clear.

The Universitat Politecnica de Catalunya (UPC, Barcelona, Spain)

From June 2008 to January 2016 nearly 800 elves have been recorded by a low-light camera in northeastern Spain. Elves occur in this region mainly over the lower-topped cold airmass maritime thunderstorms, peaking from November to January. Cloud-to-ground strokes still produce elves when maritime winter storms are carried inland, suggesting the cold season thunderstorm charge configuration favors strokes with large electromagnetic pulses. Altitudes of 389 elves were determined using optical data combined with a lightning location network. The overall median altitude was 87.1 km, near the typical OH airglow height, but average heights during individual nights ranged between 83 and 93 km. The lower elve nights (~84 km) occurred during slightly elevated geomagnetic conditions (Kp>3-, ap-index>10). Elve altitude often shifts by several kilometers during the night, apparently in response to changing background conditions in the upper mesosphere.

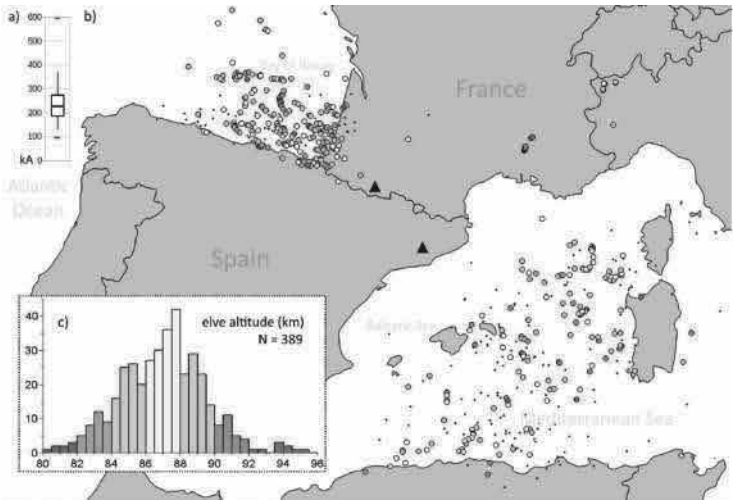

Fig. 1 a) Boxplot of the peak current of Linet-detected cloud-to-ground strokes for those elves whose altitude has been determined. b) Map with locations of detected strokes which produced elves observed from 2008-2016 by the camera in northeastern Spain (blue triangle) and Pic du Midi (black triangle). The color indicates the elve altitude according to the histogram. Black dots are Linet detections for confirmed elves without the possibility of optical verification of the stroke locations. c) Histogram of the altitudes of the events shown on the map.

The present study makes use of cloud-to-ground lightning, three-dimensional mapping from a Lightning Mapping Array and Doppler C-band radar observations to analyze the lightning trends and the underlying electrical charge structure of a large-hail bearing storm that produced important damages on the local agriculture. The analysis reported an extremely active storm, evolving through distinct phases, which stood out from a multicell structure to finally become a supercell. The onset of newer regions of convective development interacting with the main cell made the charge structure to be rather complex during some stages of this long-lived hailstorm. Evidence

suggests the presence of regions with the charge layer being inverted from that of normal, non-severe convective storms, producing predominantly positive cloud-to-ground lightning. The analysis also suggests that strong cloud signals were misclassified as low peak current single-stroke negative cloud-to-ground flashes, masking the predominant positive nature of the storm.

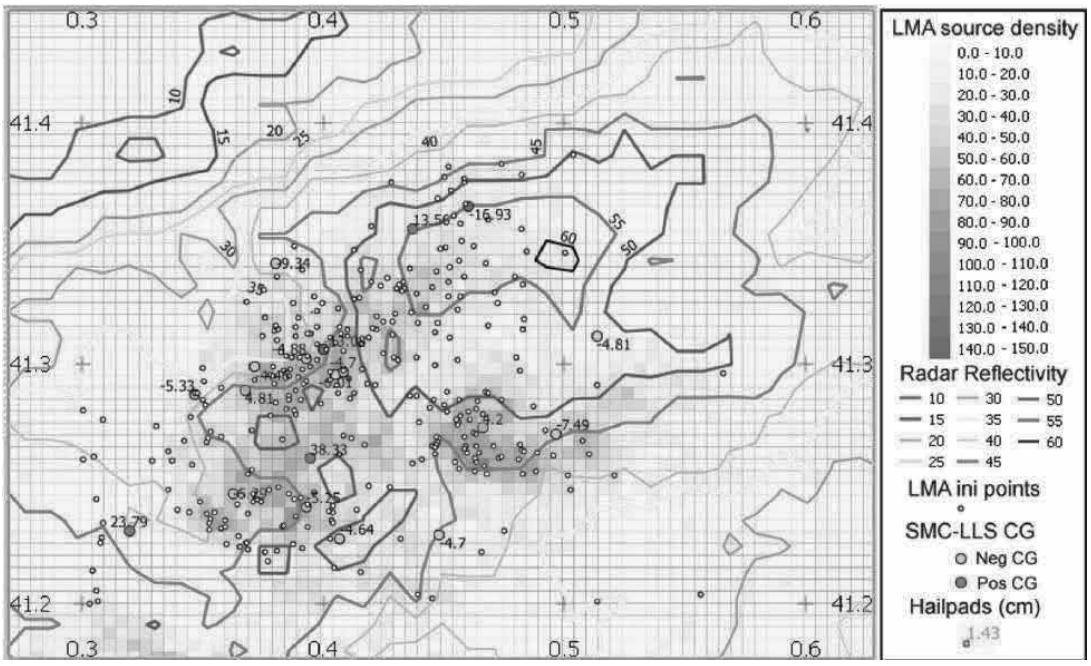

Fig. 2 Lightning mapping array (LMA) source density and maximum reflectivity at 15:24 UTC (6-min period). Plan view projection of the radar MAX product (reflectivity contour interval is of 5dBZ) overlaid on LMA source density (resolution of 0.05º). White dots correspond to the starting burst of each LMA intracloud flash. Larger dots correspond to CG strokes, its blue/red color indicating negative/positive polarity respectively. Peak currents estimated by the SMC-LLS are plotted next to each CG stroke.

Lightning is one of the major threats to multi-megawatt wind turbines and a concern for modern aircraft, due to the use of lightweight composite materials. Both wind turbines and aircraft can initiate lightning and very favorable conditions for lightning initiation occur in winter thunderstorms. Moreover, winter thunderstorms are characterized by a relatively high production of very energetic lightning. The paper reviews the different types of lightning interactions and summarizes the well-known winter thunderstorm areas. Until now comprehensive maps of global distribution of winter lightning prevalence to be used for risk assessment have been unavailable. In this paper we present the global winter lightning activity for a period of 5 years. Using lightning location data and meteorological re-analysis data, six maps are created: annual winter lightning stroke density, seasonal variation of the winter lightning and the annual number of winter thunderstorm days. In the northern hemisphere, the maps confirmed Japan to be one of the most active regions but other areas such as the Mediterranean and the US are active as well. In the southern hemisphere, Uruguay and surrounding area, the southwestern Indian Ocean

and the Tasman Sea experience the highest activity. The maps provided here can be used in the development of a risk assessment.

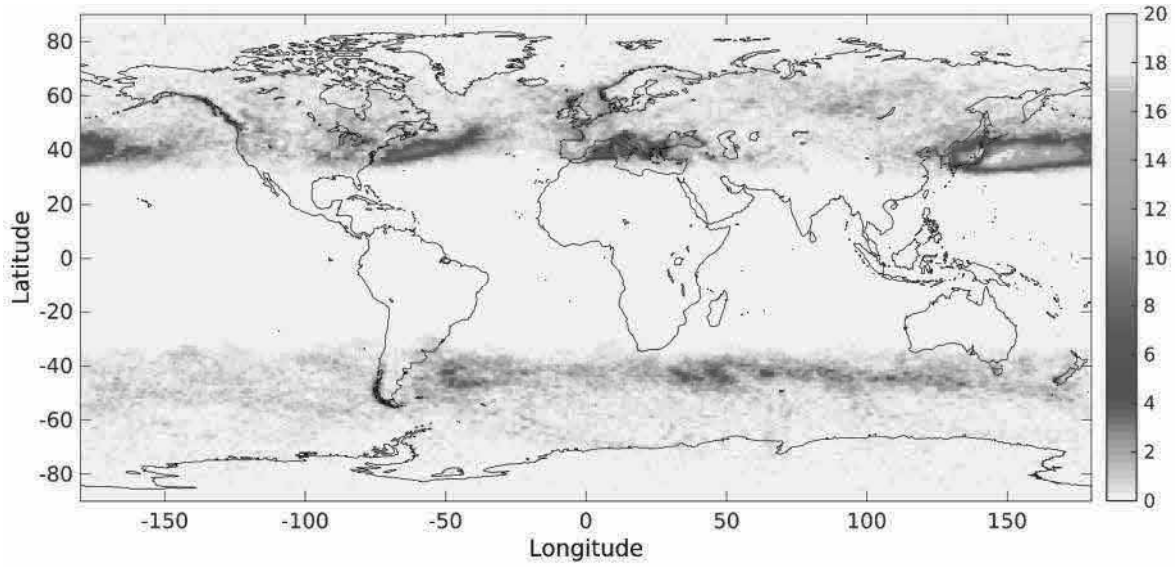

Fig. 3 Average number of winter thunderstorm days per year (T_w) for the period 2009-2013.

Attendance to the WOMEL event in Cartagena (Colombia)

From 6-8 April, 2016 we attended to the World Meeting on Lightning (WOMEL) organized by Prf. Horacio Torres (Univ. Nacional de Colombia) and his group. http://www.acofi.edu.co/womel/ The meeting allowed very interesting discussions of several atmospheric electricity and lightning protection issues. The event was a great success.

Ongoing activities

- Observations of TLE from Curaçao: A high-speed video camera system started to operate since May 2014 observing to the southwest direction over Lake Maracaibo and surrounding areas, including Catatumbo (Venezuela).
- Colombia Lightning Mapping Array (COLMA) is in operation. Before the WOMEL meeting (6-8, April 2016) Earle Williams, Jesús Alberto López and Joan Montanyà visited the Lightning Mapping Array (COLMA) network in Santa Marta (Colombia). During May Jesús Alberto López has been conducting data collection, maintenance and installed a camera at Universidad del Magdalena (Colombia).

The University of Texas at Dallas and Collaborations

Prof. Brian Tinsley and students at the University of Texas at Dallas have been working for several decades with other scientists in Australia, China and the UK on investigating the effect of atmospheric ionization and the geoelectric circuit on cloud microphysics and climate change. With Dr. Limin Zhou (East China Normal University) we have modelled the production of unipolar charge layers at the boundaries of clouds by the flow of downward current density (J_z) through

them, on its way from the ionosphere to the surface. We also modelled (Tinsley and Zhou, 2015) the effect that electric charges on aerosol particles and droplets have on the scavenging of condensation nuclei and ice-forming nuclei within clouds, which has the potential to change cloud properties such as albedo, ice production, and invigoration of updraft speeds. Such consequences are supported by data analysis, by ourselves and others, of small changes in the dynamics of winter storms that correlate with changes in the latitudinal distribution of J_z associated with solar wind variations.

Dr. Gary Burns (Australian Antarctic Division) is a collaborator who showed in 2008 that the surface pressure at Antarctic and Arctic stations correlated with the changes in overhead ionospheric potential (V_i) that determines J_z at the station locations. There were surface pressure changes of several hPa correlated independently with the changes in V_i produced by the east-west (B_y) component of the solar wind magnetic field, and with the day-to-day changes in daily average E_z due to variations in global thunderstorm activity. (The east-west magnetic component entails a north-south solar wind electric field component which raises the ionospheric potential in the Antarctic while decreasing it in the Arctic.)

Studies of these pressure changes have been extended to mid latitudes by Dr. Mai Mai Lam et al. (2013) (Reading University and British Antarctic Survey), who used global reanalysis data to evaluate the pressure changes.

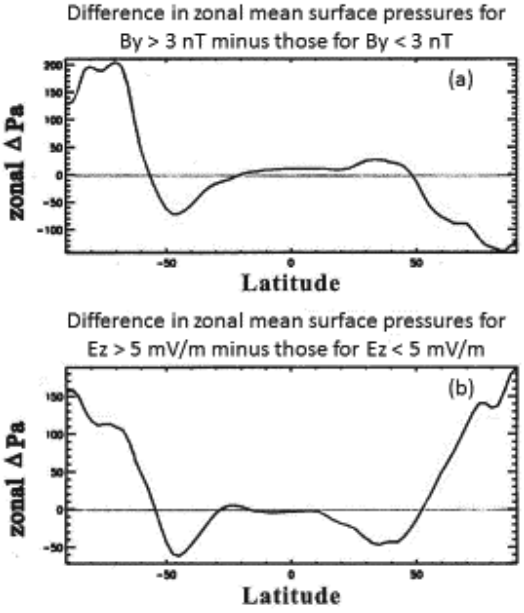

Fig. 1 Surface air pressure anomalies associated with ionospheric potential changes.

Figure 1a is a similar analysis we have made showing the zonal mean pressure response to the ionospheric potential changes produced by B_y for 1998-2001. Figure 1b is a similar analysis using E_z measurements from Vostok that were supplied by Dr. Gary Burns. (The contribution of B_y to V_i has been removed to show in Fig. 1(b) the effects of the daily variations in the thunderstorm activity (via global ionospheric potential changes) on surface pressures, which of course have the same sign of change in the Arctic as compared to the Antarctic.) The uncertainties are of order 100 Pa at the poles and less at lower latitudes.

This area of research has been recently reviewed

by Lam and Tinsley (2015) and includes a review of the modelling work we have done on the effects of electric charge on cloud microphysics. Figure 2 is from that review, and shows how the ionospheric potential change due to the solar wind B_y component is added to the diurnal (dawn-dusk) potential change due to the B_z component, illustrated in 1982 by Ralph Markson.

We are pursuing data analyses to look at seasonal and solar cycle changes in the pressure responses, as we hypothesize that they depend on seasonal changes in clouds and in the meteorological generators, and seasonal and solar cycle changes of the effect of the solar wind on polar ionospheric potentials. In addition, we continue to work on parameterizing the effect of electric charges in clouds on the scavenging of atmospheric nuclei.

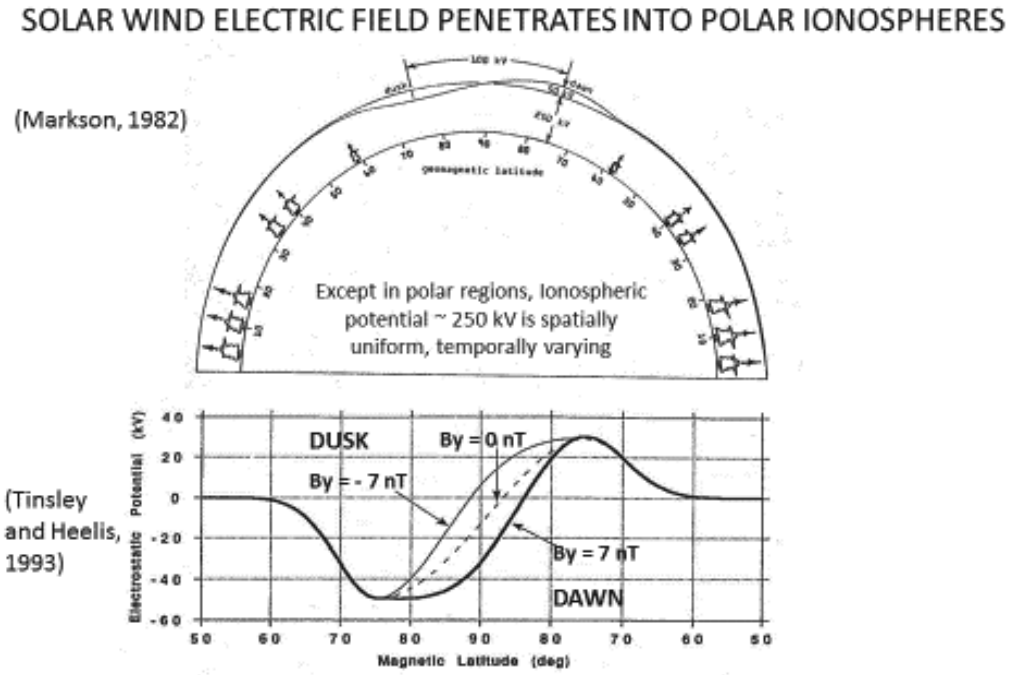

Figure 2: within 30^0 of magnetic poles solar wind (**V x B**) electric field superimposes on the background (~250 kV) potential. The B_z component gives dawn and dusk potential excursions, maximizing 15° from the magnetic poles. The B_y component maximizes at the magnetic poles.

University of Florida (Gainesville, FL, USA)

Lightning experiments and observations will continue in Summer 2016 at Camp Blanding, Florida (for the 23rd year), as well as at the Lightning Observatory in Gainesville (LOG), located at a distance of about 45 km from Camp Blanding. The two facilities are linked by a dedicated phone line. Additionally, coordinated field measurements will be performed at the Golf Course site, located at a distance of 3 km from the Camp Blanding facility. A Lightning Mapping Array (LMA) will be operated (for the 6th year) in the Camp Blanding area.

Neal Dupree (Advisor R.C. Moore) received the Outstanding Student Paper Award at the Fall 2015 AGU meeting for the paper titled "Oceanic Lightning versus Continental Lightning: VLF

Peak Current Discrepancies" and Manh Tran (Advisor V.A. Rakov) received Honorable Mention for the paper titled "New Observations of the Attachment Process in Natural Lightning". Yanan Zhu (Advisor V.A. Rakov) received Honorable Mention for the paper titled "A Study of NLDN Responses to Cloud Discharge Activity Based on Ground-Truth Data Acquired at the LOG" at the ILDC/ILMC 2016.

J. D. Hill, M. A. Uman, D. M. Jordan, T. Ngin, W. R. Gamerota, J. Pilkey, and J. Caicedo authored a paper titled "The attachment process of rocket-triggered lightning dart-stepped leaders". Time-correlated 1.54 μs high-speed video frames, channel-base current and current derivative (dI/dt), and electric field derivative (dE/dt) measurements are used to analyze the attachment process of triggered lightning dart-stepped leaders. Lengths, speeds, and durations of the upward-connecting positive leaders propagating from the launching structure are measured and calculated. The "leader burst" occurring immediately preceding the dE/dt slow front is demonstrated to be a distinctly different process from the preceding downward dart-stepped leader steps and is associated with the fast increase in channel-base current due to the initial interactions of the downward and upward leader streamer zones. Locations of the leader burst pulses are found to occur within or immediately above the connection region. Pulses superimposed on the dE/dt slow front are shown to occur after the initial connection between the downward and upward leaders and are associated with kiloampere-scale increases in the channel-base current. Subsequent fast-transition pulses are found to produce multiple kiloampere-scale increases in the channel-base current. Observed time delays between dE/dt and dI/dt peaks for slow front and fast-transition pulses confirm the existence of an elevated junction point between the downward and upward leaders. Average downward current wave speeds for fast-transition pulses are found to be a factor of 2 to 2.5 faster than those for slow-front pulses. For 51 dart-stepped leader events, the average total duration of the attachment process, starting with the initial fast current increase and ending with the peak of the final dI/dt fast-transition pulse, is measured to be 1.77 μs. The paper is published in the Journal of Geophysical Research - Atmospheres.

A. Nag (Vaisala) and V.A. Rakov authored a paper titled "A Unified Engineering Model of the First Stroke in Downward Negative Lightning". The authors presented the first unified engineering model for computing the electric field produced by a sequence of preliminary breakdown (PB), stepped leader, and return stroke processes, serving to transport negative charge to ground. They assumed that a negatively charged channel extends downward in a stepped fashion during both the PB and leader stages. Each step involves a current wave that propagates upward along the newly formed channel section. Once the leader attaches to ground, an upward propagating return stroke neutralizes the charge deposited along the channel. Model-predicted electric fields are in reasonably good agreement with simultaneous measurements at both near (hundreds of meters, electrostatic field component is dominant) and far (tens of kilometers, radiation field component is dominant) distances from the lightning channel. The authors inferred that peak currents associated with PB pulses have to be of the order of tens of kiloamperes, similar to return stroke peak currents, and that the observed increase in leader-step radiation field peaks as the leader approaches ground is at least in part due to the larger ground-corona space charge near the ground surface. The paper is published in the Journal of Geophysical Research - Atmospheres.

R. A. Wilkes, M. A. Uman, J. T. Pilkey, and D. M. Jordan authored a paper titled "Luminosity in the initial breakdown stage of cloud-to-ground and intracloud lightning". The authors presented and analyzed simultaneously measured luminosity and electric field data from the initial breakdown (IB) stage in seven cloud-to-ground (CG) and eight intracloud (IC) lightning discharges along with, in three cases, radar and Lightning Mapping Array (LMA) data taken in north-central Florida. It was found that the mean altitude (SD) of the LMA points during two CG IB stages is 5 km (600 m) and 4.3 km (250 m) and during one IC discharge is 6.2 km (550 m). The paper is published in the Journal of Geophysical Research - Atmospheres.

M. D. Tran and V. A. Rakov authored a paper titled "Attachment process in subsequent strokes and residual channel luminosity between strokes of natural lightning". The authors examined residual channel luminosity persisting over many frames (for 4.7 to 18 ms), through the pre-return-stroke frame. The residual luminosity was inferred to be associated with a stronger channel heating and a larger channel radius (and hence a lower temperature decay rate), both associated with the relatively long preceding continuing current. They also inferred ampere-scale conduction currents established in the bottom part of the channel in response to the increasing electric field of the descending subsequent-stroke leader. The paper is published in the Journal of Geophysical Research - Atmospheres.

University of São Paulo, Brazil (STORM-T Laboratory)

Prof. Rachel I. Albrecht (together with members of NOAA, NASA and UAH) authored the recent article "*Where are the lightning hotspots on Earth?*" in the Bulletin of American Meteorological Society (http://dx.doi.org/10.1175/BAMS-D-14-00193.1). The identification of Earth's Lightning Hotspots was based on 16 years (1998-2013) of total lightning flash rate density climatology from NASA's TRMM LIS satellite in very high resolution (0.1 degree). Lake Maracaibo is then named the place on Earth where most lightning occur due to very localized and persistent (297 days per year in average) development of nocturnal thunderstorms from convergent mountain-valley and land-lake breezes nearly year-round (Fig. 1). Africa holds the second place at Kabare, in Democratic Republic of Congo, and Africa is the continent with the most lightning hotspots, followed by Asia, South America, North America, and Australia. In general, most of the lightning hotspots are at or related to complex topography highlighting the importance of local features in thunderstorm development. These features are so localized that they are only recognized when looking at the fine scales of the interaction between wind and complex terrain that leads to cloud development.

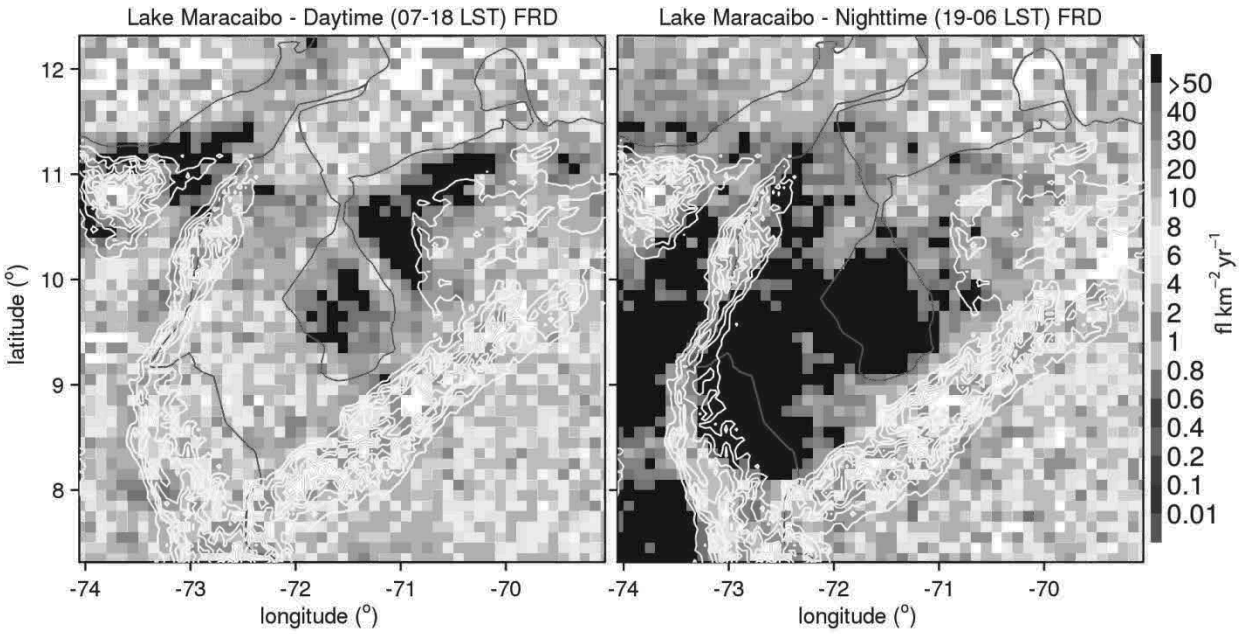

Fig. 1. Daytime (07-18 LST) and nighttime (19-06) flash rate density (fl km^2 yr^{-1}) at Lake Maracaibo, Venezuela. White lines are elevation from 500 to 3000 m in 500 m intervals, and gray lines are country physical boundaries. Adapted from Albrecht et al. (2016) (http://dx.doi.org/10.1175/BAMS-D-14-00193.1).

With the recent end of GoAmazon (http://campaign.arm.gov/goamazon2014/) and CHUVA Project (http://chuvaproject.cptec.inpe.br) field campaigns, Prof. Albrecht and Prof. Carlos A. Morales continue the analysis of cloud-aerosol-precipitation interactions in deep convection identifying and quantifying local (topography and land cover), thermodynamical and large-scale features responsible for thunderstorm development and microphysical differences among the Amazon basin. Thanks to a CNPq proposal, it was possible to deploy the LINET network around Manaus during the second GoAmazon intensive period (IOP2) and ACRIDICON-CHUVA field experiments (September-October – 2014), Fig. 2. In summary (Fig. 3), most of the lightning activity occurred on the east side of Rio Negro River, north and northeast of Manaus, mainly due to afternoon thunderstorms with some exceptions on few days that showed the presence large-scale squall lines that crossed during nighttime. It is important to note that this region holds Brazil's first total lightning hotspot according to the TRMM LIS climatological study present in Albrecht et al. (2016) and STARNET climatology (2015) (Fig. 4).

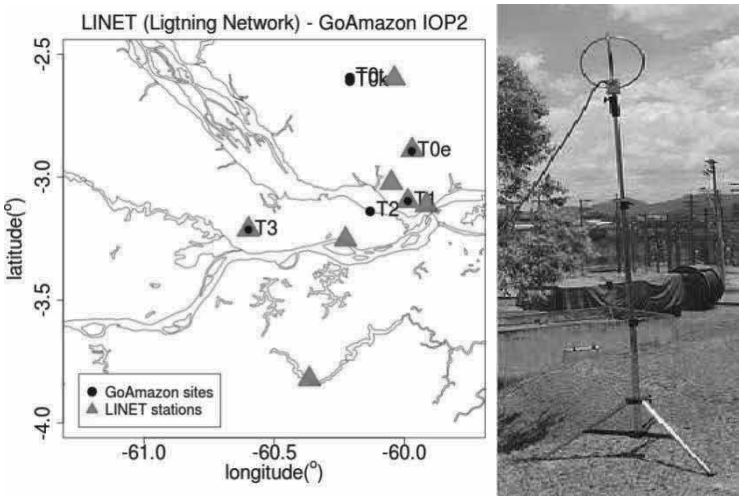

Fig. 2 (left) Location of the 8 LINET sensors over Manaus region during GoAmazon IOP2, CHUVA Project and ACRIDICON-CHUVA field experiments (dark blue lines are the rivers physical boundaries); (right) photo of a LINET sensor.

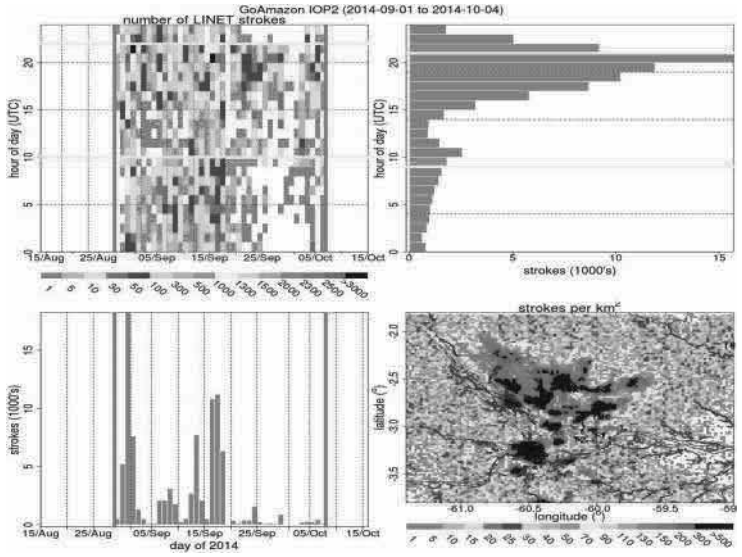

Fig. 3 Summary of LINET lightning occurrence during GoAmazon IOP2. (upper left) Number of lighting strokes by hour of the day and day of the year, (upper right) histogram of lightning occurrence by hour of the day, (lower left) histogram of lightning occurrence by day of the year, and (lower right) spatial distribution of lighting strokes (dark blue lines are the rivers physical boundaries).

After 9 years of continuous measurements STARNET (Sferics Timing and Ranging Network) reaches a maturity to monitor the lightning activity in South America, Figure 4. The recent results presented on ICAE-2014 and SIPDA-2015 show that STARNET has a similar performance of GLD360 and agree with the recent work of Albrecht et al. (2016) on LIS data in the position and intensity of the lightning hotspots in South America, i.e., Lake Maracaibo and Colombia. In 2015, more than 53 million sferics were detected by STARNET and more than 58% were observed in Brazil. The top 5 lightning hotspots in Brazil were in Corumbá (Mato Grosso do Sul), São Feliz do Xingu and Altamira (Pará) and Tapauã (Amazon), and Legal Amazon holds more than

60% of the observed lightning in Brazil.
During this last austral summer (2015/2016), we have deployed 8 LINET sensors around the metropolitan area of São Paulo city in a cooperation with DLR and Nowcast. This project seeks a better interpretation of how thunderstorms change as propagate in larger urban area affected by topography and sea breeze. Moreover, the PhD student Diego F. Del Rio Truillo, from Universidad Nacional de Colombia at Manizales and advised by Professor Camilo Younes, is visiting our laboratory for 6 months to collaborate in an effort to understand the role of pollution and local circulation on the lightning activity in Colombia.

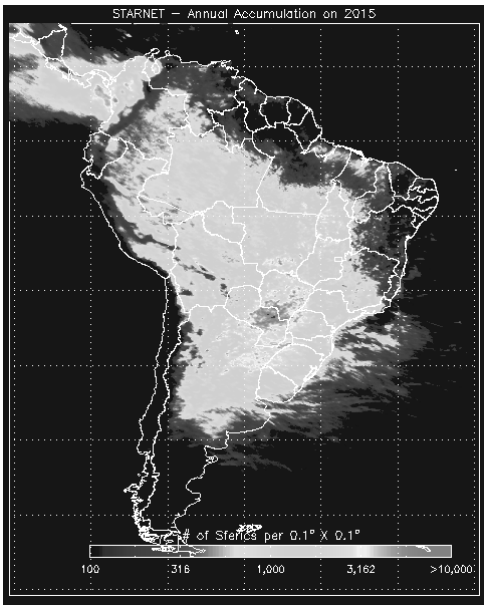

Fig. 4 Sferics annual distribution at 0.1 x 0.1º grid box during 2015.

Vaisala

ILDC/ILMC Conference Summary
Vaisala sponsored the 24th International Lightning Detection Conference (ILDC) and the 6th International Lightning Meteorology Conference (ILMC) in San Diego, California in late April 2016. A total of 125 attendees were at the meeting where over 100 presentations were made based on abstracts from 16 countries. Topics ranged from basic physics of lightning through the applications of lightning data, as well as topics bridging these fields of study. Substantial interactions occurred during the meetings as well as during the breaks and other activities. The Krider Scholarship was awarded to outstanding presentations by two students: Daile Zhang (University of Arizona, USA) and Miguel Guimaraes (Federal University of Minas Gerais, Brazil). The location of the next ILDC/ILMC conferences planned for February 2018 will be announced in the near future. Dr. Larry Carey from the University of Alabama-Huntsville and Dr. Marcelo Saba from INPE, Brazil will Co-Chair the conferences.
"A summary of recent national-scale lightning fatality studies"by Holle, R.L.

There is a major difference in population-weighted lightning fatality rates between the lower fatality rates in developed countries and the higher fatality rates in developing countries. The large decrease in annual rates of population-weighted lightning fatalities in the United States is described over the last century. A similar large reduction in lightning fatality rates has occurred during recent years in Australia, Canada, Japan, and Western Europe, where there has also been a change from a mainly rural agricultural society to a primarily urban society. An important accompanying aspect of the lower casualty rates has been the widespread availability of lightning-safe large buildings and fully enclosed metal-topped vehicles, as well as much greater awareness of the lightning threat, better medical treatment, and availability of real-time lightning information. However, lightning exposure for many people in lesser-developed countries is similar to that of a century ago in developed countries. The number of people living in these areas may be increasing in number, so the number of people killed by lightning may be increasing globally due to these socioeconomic factors. It can be difficult to locate national lightning fatality data because of their mainly obscure publication sources. The present paper synthesizes lightning fatality data from 23 published national-scale studies during periods ending in 1979 and later, and maps these fatality rates per million by continent.

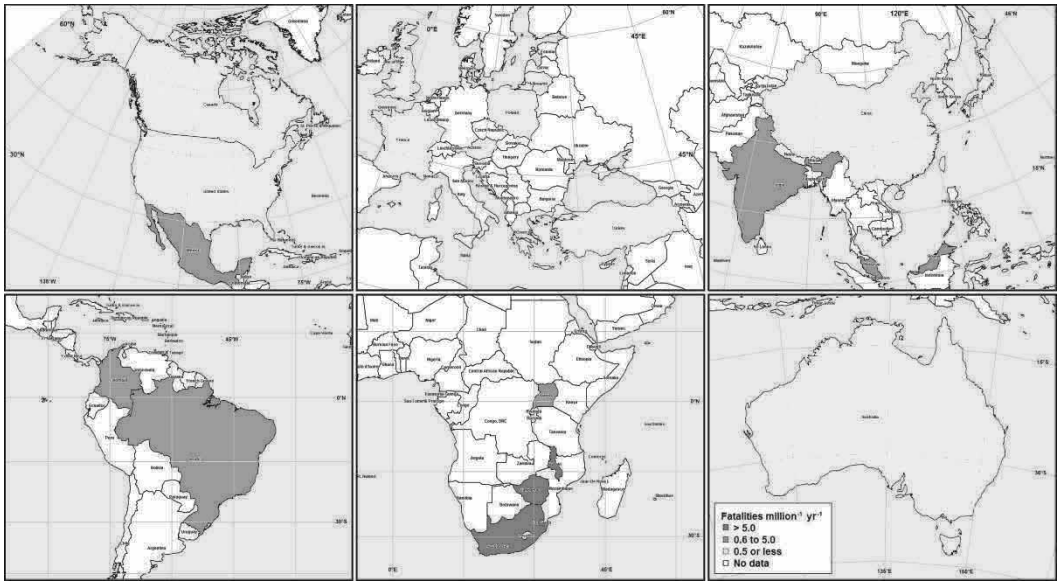

Fig. 1 National lightning fatality rate per million people per year by continent. Red shading indicates rate > 5.0 fatalities per million per year, orange is 0.6–5.0, and yellow is 0.5 or less. White indicates no national summaries have been published for datasets ending in 1979 or later.

RECENT PUBLICATIONS

This list of references is not exhaustive. It includes only papers published during the last six months provided by the authors or found from an on-line research in journal websites. Some references of papers very soon published have been provided by their authors and included in the list. The papers in review process, the papers from Proceedings of Conference are not included.

Adachi T., M. Sato, T. Ushio, A. Yamazaki, M. Suzuki, M. Kikuchi, Y. Takahashi, U. S. Inan, I. Linscott, Y. Hobara, H. U. Frey, S. B. Mende, A. B. Chen, R.-R. Hsu, K. Kusunoki. 2016. Identifying the occurrence of lightning and transient luminous events by nadir spectrophotometric observation. J. Atmos. Sol-terr. Phy., 145: 85–97.

Adhikari P. B., S. Sharma, K. Baral. 2016. Features of positive ground flashes observed in Kathmandu Nepal. J. Atmos. Sol-terr. Phy., 145: 106–113.

Albrecht R. I., S. J. Goodman, D. E. Buechler, R. J. Blakeslee, and H. J. Christian. 2016. Where are the lightning hotspots on Earth? Bull. Am. Meteorol. Soc., in press, doi: http://dx.doi.org/10.1175/BAMS-D-14-00193.1.

Allen J. T., E. R. Allen. 2016. A review of severe thunderstorms in Australia. Atmos. Res., 178–179: 347–366.

Azadifar M., F. Rachidi, M. Rubinstein, M. Paolone, G. Diendorfer, H. Pichler, W. Schulz, D. Pavanello and C. Romero. 2016. Evaluation of the performance characteristics of the European Lightning Detection Network EUCLID in the Alps region for upward negative flashes using direct measurements at the instrumented Säntis Tower. J. Geophys. Res. Atmos., 121(2): 595–606.

Baba Y. and V. A. Rakov. Electromagnetic Computation Methods for Lightning Surge Protection Studies. Wiley-IEEE Press, 320 p., 2016, ISBN: 978-1-118-27563-4.

Baharudin Z. A., V. Cooray, M. Rahman, P. Hettiarachchi, N. A. Ahmad. 2016. On the characteristics of positive lightning ground flashes in Sweden. J. Atmos. Sol-terr. Phy., 138–139: 106–111.

Barth M. C., M. M. Bela, A. Fried, P. O. Wennberg, J. D. Crounse, J. M. St. Clair, N. J. Blake, D. R. Blake, C. R. Homeyer, W. H. Brune, L. Zhang, J. Mao, X. Ren, T. B. Ryerson, I. B. Pollack, J. Peischl, R. C. Cohen, B. A. Nault, L. G. Huey, X. Liu and C. A. Cantrell. 2016. Convective transport and scavenging of peroxides by thunderstorms observed over the central U.S. during DC3. J. Geophys. Res. Atmos., 29 APR 2016, DOI: 10.1002/2015JD024570.

Boggs L. D., N. Liu, M. Splitt, S. Lazarus, C. Glenn, H. Rassoul and S. A. Cummer. 2016. An analysis of five negative sprite-parent discharges and their associated thunderstorm charge structures. J. Geophys. Res. Atmos., 121(2): 759–784.

Bór J., B. Ludván, A. Novák and P. Steinbach. 2016. Systematic deviations in source direction estimates of Q-bursts recorded at Nagycenk, Hungary. J. Geophys. Res. Atmos., 9 MAY 2016, DOI: 10.1002/2015JD024712.

Caicedo J. A., C. Biagi, M. A. Uman, D. M. Jordan and B. Hare. 2016. Return stroke current reflections in rocket-triggered lightning. J. Geophys. Res. Atmos., 121(6): 2973–2993.

Celestin S., W. Xu and V. P. Pasko. 2015. Variability in fluence and spectrum of high-energy photon bursts produced by lightning leaders. J. Geophys. Res. Space Physics, 120(12): 10,712–10,723.

Cen J., P. Yuan, S. Xue, X. Wang. 2015. Spectral characteristics of lightning dart leader propagating in long path. Atmos. Res.,

RECENT PUBLICATIONS

164–165: 95–98.

Chronis T., T. Lang, W. Koshak, R. Blakeslee, H. Christian, E. McCaul and J. Bailey. 2015. Diurnal characteristics of lightning flashes detected over the São Paulo lightning mapping array. J. Geophys. Res. Atmos., 120(23): 11,799–11,808.

Chronis T., W. Koshak and E. McCaul. 2016. Why do oceanic negative cloud-to-ground lightning exhibit larger peak current values? J. Geophys. Res. Atmos., 22 APR 2016, DOI: 10.1002/2015JD024129.

Cimarelli C., M. A. Alatorre-Ibargüengoitia, K. Aizawa, A. Yokoo, A. Díaz-Marina, M. Iguchi and D. B. Dingwell. 2016. Multiparametric observation of volcanic lightning: Sakurajima Volcano, Japan. Geophys. Res. Lett., 6 MAY 2016, DOI: 10.1002/2015GL067445.

Conti A. D., F. H. Silveira, S. Visacro, T. C.M. Cardoso. 2015. A review of return-stroke models based on transmission line theory. J. Atmos. Sol-terr. Phy., 136: 52–60.

Cooray V. 2015. On the mimimum length of leader channel and the minimum volume of space charge concentration necessary to initiate lightning flashes in thunderclouds. J. Atmos. Sol-terr. Phy., 136: 39–45.

Cooray V. 2016. Corrigendum to: "On the mimimum length of leader channel and the minimum volume of space charge concentration necessary to initiate lightning flashes in thunderclouds" [J. Atmos. Sol.-Terr. Phys. 136 (2015) 39–45]. J. Atmos. Sol-terr. Phy., 142: 152.

Cooray V. A return stroke model based purely on the current dissipation concept. J. Atmos. Sol-terr. Phy., 136: 61–65.

Czernecki B., M. Taszarek, L. Kolendowicz, J. Konarski. 2016. Relationship between human observations of thunderstorms and the PERUN lightning detection network in Poland. Atmos. Res., 167: 118–128.

Dong C., P. Yuan, J. Cen, X. Wang, Y. Mu. 2016. The heat transfer characteristics of lightning return stroke channel. Atmos. Res., 178–179: 1–5.

Eaton A. R. V., Á. Amigo, D. Bertin, L. G. Mastin, R. E. Giacosa, J. González, O. Valderrama, K. Fontijn and S. A. Behnke. 2016. Volcanic lightning and plume behavior reveal evolving hazards during the April 2015 eruption of Calbuco volcano, Chile. Geophys. Res. Lett., 43(7): 3563–3571.

Galanaki E., V. Kotroni, K. Lagouvardos, A. Argiriou. 2016. A ten-year analysis of cloud-to-ground lightning activity over the Eastern Mediterranean region. Atmos. Res., 166: 213–222.

García M. M., J. R. Martín, L. R. Soriano, F. P. Dávila. 2015. Observed impact of land uses and soil types on cloud-to-ground lightning in Castilla-Leon (Spain). Atmos. Res., 166: 233–238.

Gjesteland T., N. Østgaard, S. Laviola, M. M. Miglietta, E. Arnone, M. Marisaldi, F. Fuschino, A. B. Collier, F. Fabró and J. Montanya. 2015. Observation of intrinsically bright terrestrial gamma ray flashes from the Mediterranean basin. J. Geophys. Res. Atmos., 120(23): 12,143–12,156.

Gordillo-Vázquez F. J., A. Luque and C. Haldoupis. 2016. Upper D region chemical kinetic modeling of LORE relaxation times. J. Geophys. Res. Space Physics, 15 APR 2016, DOI: 10.1002/2015JA021408.

Gunasekara T.A.L.N., M. Fernando, U. Sonnadara, V. Cooray. 2016. Characteristics of Narrow Bipolar Pulses observed from lightning in Sri Lanka. J. Atmos. Sol-terr. Phy., 138–139: 66–73.

Gurevich A.V., V.P. Antonova, A.P. Chubenko, A.N. Karashtin, O.N. Kryakunova, V.Yu.

RECENT PUBLICATIONS

Lutsenko, G.G. Mitko, V.V. Piskal, M.O. Ptitsyn, V.A. Ryabov, A.L. Shepetov, Yu.V. Shlyugaev, W.M. Thu, L.I. Vildanova, K.P. Zybin. 2015. The time structure of neutron emission during atmospheric discharge. Atmos. Res., 164–165: 339–346.

Hill J. D., M. A. Uman, D. M. Jordan, T. Ngin, W. R. Gamerota, J. Pilkey and J. Caicedo. 2016. The attachment process of rocket-triggered lightning dart-stepped leaders. J. Geophys. Res. Atmos., 121(2): 853–871.

Holle R. L. 2016. A summary of recent national-scale lightning fatality studies. Weather, Climate, and Society, 8: 35-42.

Huntrieser H., M. Lichtenstern, M. Scheibe, H. Aufmhoff, H. Schlager, T. Pucik, A. Minikin, B. Weinzierl, K. Heimerl, I. B. Pollack, J. Peischl, T. B. Ryerson, A. J. Weinheimer, S. Honomichl, B. A. Ridley, M. I. Biggerstaff, D. P. Betten, J. W. Hair, C. F. Butler, M. J. Schwartz and M. C. Barth. 2016. Injection of lightning-produced NOx, water vapor, wildfire emissions, and stratospheric air to the UT/LS as observed from DC3 measurements. J. Geophys. Res. Atmos., 1 APR 2016, DOI: 10.1002/2015JD024273.

Hussein A.M., S. Kazazi, M. Anwar, M. Yusouf, P. Liatos. 2016. Characteristics of the most intense lightning storm ever recorded at the CN tower. J. Atmos. Sol-terr. Phy., In Press, Accepted Manuscript, Available online 7 May 2016.

Iordanidou V., A.G. Koutroulis, I.K. Tsanis. 2016. Investigating the relationship of lightning activity and rainfall: A case study for Crete Island. Atmos. Res., 172–173: 16–27.

Ishtiaq P. M., S. Mufti, M. A. Darzi, T. A. Mir and G. N. Shah. 2016. Observation of 2.45 MeV neutrons correlated with natural atmospheric lightning discharges by Lead-Free Gulmarg Neutron Monitor. J. Geophys. Res. Atmos., 121(2): 692–703.

Jánský J. and V. P. Pasko. 2015. Effects of conductivity perturbations in time-dependent global electric circuit model. J. Geophys. Res. Space Physics, 120(12): 10,654–10,668.

Jiang R., X. Qie, Z. Wang, H. Zhang, G. Lu, Z. Sun, M. Liu and X. Li. 2015. Characteristics of lightning leader propagation and ground attachment. J. Geophys. Res. Atmos., 120(23): 11,988–12,002.

Karagiannidis A., K. Lagouvardos, V. Kotroni. 2016. The use of lightning data and Meteosat infrared imagery for the nowcasting of lightning activity. Atmos. Res., 168: 57–69.

Kolmašová I., O. Santolík, T. Farges, S. A. Cummer, R. Lán and L. Uhlíř. 2016. Subionospheric propagation and peak currents of preliminary breakdown pulses before negative cloud-to-ground lightning discharges. Geophys. Res. Lett., 43(3): 1382–1391.

Kostinskiy A. Y., V. S. Syssoev, E. A. Mareev, V. A. Rakov, M. G. Andreev, N. A. Bogatov, L. M. Makal'sky, D. I. Sukharevsky, A. S. Aleshchenko, V. E. Kuznetsov, M. V. Shatalina. 2015. Electric discharges produced by clouds of charged water droplets in the presence of moving conducting object. J. Atmos. Sol-terr. Phy., 135: 36–41.

Kumar U. 2015. Role of upward leaders in modifying the induced currents in solitary down-conductors during a nearby lightning strike to ground. J. Atmos. Sol-terr. Phy., 134: 30–40.

Kuo C. L., H. T. Su and R. R Hsu. 2015. The blue luminous events observed by ISUAL payload on board FORMOSAT-2 satellite. J. Geophys. Res. Space Physics, 120(11): 9795–9804.

Liu N., L. D. Boggs and S. A. Cummer. 2016. Observation-constrained modeling of the ionospheric impact of negative sprites. Geophys. Res. Lett., 43(6): 2365–2373.

RECENT PUBLICATIONS

Liu N., M. G. McHarg, H. C. Stenbaek-Nielsen. 2015. High-altitude electrical discharges associated with thunderstorms and lightning. J. Atmos. Sol-terr. Phy., 136: 98–118.

Lu G., S. A. Cummer, Y. Tian, H. Zhang, F. Lyu, T. Wang, M. A. Stanley, J. Yang and W. A. Lyons. 2016. Sprite produced by consecutive impulse charge transfers following a negative stroke: Observation and simulation. J. Geophys. Res. Atmos., 22 APR 2016, DOI: 10.1002/2015JD024644.

Lu W., Q. Qi, Y. Ma, L. Chen, X. Yan, V. A. Rakov, D. Wang, Y. Zhang. 2016. Two basic leader connection scenarios observed in negative lightning attachment process. High Volt., 1(1): 11–17.

Lu W., Y. Gao, L. Chen, Q. Qi, Y. Ma, Y. Zhang, S. Chen, X. Yan, C. Chen, Y. Zhang. 2015. Three-dimensional propagation characteristics of the leaders in the attachment process of a downward negative lightning flash. J. Atmos. Sol-terr. Phy., 136: 23–30.

Madhuri N. K., D. Siingh. 2016. The atmospheric electrical index for ENSO modoki: Is ENSO modoki one of the factors responsible for the warming trend slowdown?, Scientific Reports, 6: 1–10.

Mäkelä A., J. Mäkelä, J. Haapalainen, N. Porjo. 2016. The verification of lightning location accuracy in Finland deduced from lightning strikes to trees. Atmos. Res., 172–173: 1–7.

Marisaldi M., A. Argan, A. Ursi, T. Gjesteland, F. Fuschino, C. Labanti, M. Galli, M. Tavani, C. Pittori, F. Verrecchia, F. D'Amico, N. Østgaard, S. Mereghetti, R. Campana, P.W. Cattaneo, A. Bulgarelli, S. Colafrancesco, S. Dietrich, F. Longo, F. Gianotti, P. Giommi, A. Rappoldi, M. Trifoglio and A. Trois. 2015. Enhanced detection of terrestrial gamma-ray flashes by AGILE. Geophys. Res. Lett., 42(21): 9481–9487.

Marzuki, H. Hashiguchi, T. Kozu, T. Shimomai, Y. Shibagaki, Y. Takahashi. 2016. Precipitation microstructure in different Madden–Julian Oscillation phases over Sumatra. Atmos. Res., 168: 121–138.

Matsangouras I.T., P.T. Nastos, J. Kapsomenakis. 2016. Cloud-to-ground lightning activity over Greece: Spatio-temporal analysis and impacts. Atmos. Res., 169: 485–496.

McTague L. E., S. A. Cummer, M. S. Briggs, V. Connaughton, M. Stanbro and G. Fitzpatrick. 2015. A lightning-based search for nearby observationally dim terrestrial gamma ray flashes. J. Geophys. Res. Atmos., 120(23): 12,003–12,017.

Miranda F.J., S.R. Sharma. 2016. Multifractal analysis of lightning channel for different categories of lightning. J. Atmos. Sol-terr. Phy., 145: 34–44.

Mona T., Á. Horváth, F. Ács. 2016. A thunderstorm cell-lightning activity analysis: The new concept of air mass catchment. Atmos. Res., 169: 340–344.

Montanyà J., F. Fabró, O. van der Velde, V. March, E. R. Williams, N. Pineda, D. Romero, G. Solà, M., Freijo. 2016. Global Distribution of Winter Lightning: a threat to wind turbines and aircraft. Nat. Hazards Earth Syst. Sci. Discuss., doi:10.5194/nhess-2015-302.

Montanyà J., F. Fabró, V. March, O. van der Velde, G. Solà, D. Romero, O. Argemí. 2015. X-rays and microwave RF power from high voltage laboratory sparks. J. Atmos. Sol-terr. Phy., 136: 94–97.

Mu Y., P. Yuan, X. Wang, C. Dong. 2016. Temperature distribution and evolution characteristic in lightning return stroke channel. J. Atmos. Sol-terr. Phy., 145: 98–105.

MuñozÁ.G., J. Díaz-Lobatón, X. Chourio, M.J. Stock. 2016. Seasonal prediction of lightning activity in North Western Venezuela:

RECENT PUBLICATIONS

Large-scale versus local drivers. Atmos. Res., 172–173:147–162.

Nag A. and V. A. Rakov, 2016. A unified engineering model of the first stroke in downward negative lightning. J. Geophys. Res. Atmos., 121(5): 2188–2204.

Østgaard N., B. E. Carlson, R. S. Nisi, T. Gjesteland, Ø. Grøndahl, A. Skeltved, N. G. Lehtinen, A. Mezentsev, M. Marisaldi and P. Kochkin. 2016. Relativistic electrons from sparks in the laboratory. J. Geophys. Res. Atmos., 121(6): 2939–2954.

Østgaard N., K. H. Albrecthsen, T. Gjesteland and A. Collier. 2015. A new population of terrestrial gamma-ray flashes in the RHESSI data. Geophys. Res. Lett., 42(24): 10,937–10,942.

Owens M. J., C. J. Scott, A. J. Bennett, S. R. Thomas, M. Lockwood, R. G. Harrison and M. M. Lam. 2015. Lightning as a space-weather hazard: UK thunderstorm activity modulated by the passage of the heliospheric current sheet. Geophys. Res. Lett., 42(22): 9624–9632.

Pineda N., T. Rigo, J. Montanyà, O. A. van der Velde. 2016. Charge structure analysis of a severe hailstorm with predominantly positive cloud-to-ground lightning. Atmos. Res., 178–179: 31–44.

Proestakis E., S. Kazadzis, K. Lagouvardos, V. Kotroni, A. Kazantzidis. 2016. Lightning activity and aerosols in the Mediterranean region. Atmos. Res., 170: 66–75.

Pytharoulis I., S. Kotsopoulos, I. Tegoulias, S. Kartsios, D. Bampzelis, T. Karacostas. 2016. Numerical modeling of an intense precipitation event and its associated lightning activity over northern Greece. Atmos. Res., 169: 523–538.

Qi Q., W. Lu, Y. Ma, L. Chen, Y. Zhang, V. A. Rakov. 2016. High-speed video observations of the fine structure of a natural negative stepped leader at close distance. Atmos. Res., 178–179: 260–267.

Qiu S., Z. Jiang, L. Shi, Z. Niu, P. Zhang. 2015. Characteristics of negative lightning leaders to ground observed by TVLS. J. Atmos. Sol-terr. Phy., 136: 31–38.

Quick M. G, E. P. Krider. 2015. Optical emission and peak electromagnetic power radiated by negative return strokes in rocket-triggered lightning. J. Atmos. Sol-terr. Phy., 136: 80–85.

Rakov V. A. Fundamentals of Lightning. Cambridge University Press, 257 p., 2016, ISBN: 9781107072237.

Shao X.-M. 2016. Generalization of the lightning electromagnetic equations of Uman, McLain, and Krider based on Jefimenko equations. J. Geophys. Res. Atmos., 121(7): 3363–3371.

Shi Z., Y.B. Tan, H.Q. Tang, J. Sun, Y. Yang, L. Peng, X.F. Guo. 2015. Aerosol effect on the land-ocean contrast in thunderstorm electrification and lightning frequency. Atmos. Res., 164–165: 131–141.

Shmatov M. L. 2015. Possible scenarios for the initial acceleration of electrons of the core of ball lightning. J. Plasma Phys., 81(6): 905810607.

Siingh D., R.P. Singh, S. Kumar, T. Dharmaraj, A. K. Singh, A. K. Singh, M.N. Patil, S. Singh. 2015. Lightning and middle atmospheric discharges in the atmosphere. J. Atmos. Sol-terr. Phy., 134:78–101.

Silva C. L. da, R. A. Merrill and V. P. Pasko. 2016. Mathematical constraints on the use of transmission line models to investigate the preliminary breakdown stage of lightning flashes. Radio Sci., 4 MAY 2016, DOI: 10.1002/2015RS005853.

Smorgonskiy A., A. Tajalli, F. Rachidi, M. Rubinstein, G. Diendorfer, H. Pichler. 2015. An analysis of the initiation of upward flashes from tall towers with particular reference to Gaisberg and Säntis Towers. J. Atmos. Sol-terr.

RECENT PUBLICATIONS

Phy., 136: 46–51.

Somu V. B., V. A. Rakov, M. A. Haddad, S.A. Cummer. 2015. A study of changes in apparent ionospheric reflection height within individual lightning flashes. J. Atmos. Sol-terr. Phy., 136: 66–79.

Soula S., J. K. Kasereka, J.F. Georgis, C. Barthe. 2016. Lightning climatology in the Congo Basin. Atmos. Res., 178–179: 304–319.

Stolzenburg M., T. C. Marshall and P. R. Krehbiel. 2015. Initial electrification to the first lightning flash in New Mexico thunderstorms. J. Geophys. Res. Atmos., 120(21): 11,253–11,276.

Sun Z., X. Qie, M. Liu, R. Jiang, Z. Wang and H. Zhang. 2016. Characteristics of a negative lightning with multiple-ground terminations observed by a VHF lightning location system. J. Geophys. Res. Atmos., 121(1): 413–426.

Tan Y. B., L. Peng, Z. Shi, H. R. Chen. 2016. Lightning flash density in relation to aerosol over Nanjing (China). Atmos. Res., 174–175: 1–8.

Tatsis G., C. Votis, V. Christofilakis, P. Kostarakis, V. Tritakis, C. Repapis. 2015. A prototype data acquisition and processing system for Schumann resonance measurements. J. Atmos. Sol-terr. Phy., 135: 152–160.

Thang T. H., Y. Baba, V. A. Rakov, A. Piantini. 2015. Lightning-induced voltages in the presence of nearby buildings: FDTD simulation vs. small-scale experiment. IEEE Trans. on EMC, 57(6): 1601–1607.

Tian Y., X. Qie, G. Lu, R. Jiang, Z. Wang, H. Zhang, M. Liu, Z. Sun, G. Feng. 2016. Characteristics of a bipolar cloud-to-ground lightning flash containing a positive stroke followed by three negative strokes. Atmos. Res., 176–177: 222–230.

Tonev P. T., P. I.Y. Velinov. 2016. Influence of solar activity on red sprites and on vertical coupling in the system stratosphere–mesosphere. J. Atmos. Sol-terr. Phy., 141: 27–38.

Tonev P.T., P.I.Y. Velinov. 2016. Vertical coupling between troposphere and lower ionosphere by electric currents and fields at equatorial latitudes. J. Atmos. Sol-terr. Phy., 141: 39–47.

Tran M. D. and V. A. Rakov. 2015. Attachment process in subsequent strokes and residual channel luminosity between strokes of natural lightning. J. Geophys. Res. Atmos., 120(23): 12,248–12,258.

Tran M.D., V.A. Rakov, S. Mallick, J.R. Dwyer, A. Nag, S. Heckman. 2015. A terrestrial gamma-ray flash recorded at the Lightning Observatory in Gainesville, Florida. J. Atmos. Sol-terr. Phy., 136: 86–93.

Velde O. A. van der and J. Montanyà. 2016. Statistics and variability of the altitude of elves. Geophys. Res. Lett., 7 MAY 2016, DOI: 10.1002/2016GL068719.

Venugopal V., K. Virts, J. Sukhatme, J.M. Wallace, B. Chattopadhyay. 2016. A comparison of the fine-scale structure of the diurnal cycle of tropical rain and lightning. Atmos. Res., 169: 515–522.

Wang F., Y. Zhang, D. Zheng, et al. 2015. Impact of the vertical velocity field on charging processes and charge separation in a simulated thunderstorm. J. Meteor. Res., 29(2), 328–343.

Wang F., Y. Zhang, D. Zheng. 2015. Impact of updraft on neutralized charge rate by lightning in thunderstorms: A simulation case study. J. Meteor. Res., 29(6), 997–1010.

Wang F., Y. Zhang, H. Liu, W. Yao, Q. Meng. 2016. Characteristics of cloud-to-ground lightning strikes in the stratiform regions of mesoscale convective systems. Atmos. Res., 178–179: 207–216.

Wang H., F. Guo, T. Zhao, M. Qin, L. Zhang. 2016. A numerical study of the positive

RECENT PUBLICATIONS

cloud-to-ground flash from the forward flank of normal polarity thunderstorm. Atmos. Res., 169: 183–190.

Wang J., S. Zhou, B. Yang, X. Meng, B. Zhou. 2016. Nowcasting cloud-to-ground lightning over Nanjing area using S-band dual-polarization Doppler radar. Atmos. Res., 178–179: 55–64.

Wang Y., X. Qie, D. Wang, M. Liu, D. Su, Z. Wang, D. Liu, Z. Wu, Z. Sun, Y. Tian. 2016. Beijing Lightning Network (BLNET) and the observation on preliminary breakdown processes. Atmos. Res., 171: 121–132.

Wilkes R. A., M. A. Uman, J. T. Pilkey and D. M. Jordan. 2016. Luminosity in the initial breakdown stage of cloud-to-ground and intracloud lightning. J. Geophys. Res. Atmos., 121(3): 1236–1247.

Williams E. R., E. V. Mattos and L. A. T. Machado. 2016. Stroke multiplicity and horizontal scale of negative charge regions in thunderclouds. Geophys. Res. Lett., 7 MAY 2016, DOI: 10.1002/2016GL068924.

Xie Y., J. Wu, X. Liu, T. Zhang, Y. Xie, Y. Xu, D. Zhao. 2015. Characteristics of cloud-to-ground lightning activity in hailstorms over Yunnan province. J. Atmos. Sol-terr. Phy., 136: 2–7

Yang L., J. Smith, M. L. Baeck, B. Smith, F. Tian and D. Niyogi. 2016. Structure and evolution of flash flood producing storms in a small urban watershed. J. Geophys. Res. Atmos., 121(7): 3139–3152.

Yaniv R., Y. Yair, C. Price, S. Katz. 2016. Local and global impacts on the fair-weather electric field in Israel. Atmos. Res., 172–173: 119–125.

Yu J.L., Y.D. Fan, J.G. Wang, R.H. Qi, M. Zhou, L. Cai, M.J. Cui, Z.J. Yuan. 2016. Characteristics of the horizontal electric field associated with nearby lightning return strokes. J. Atmos. Sol-terr. Phy., In Press, Available online 22 February 2016.

Yuan T., Y. Di, K. Qie. 2016. Variability of lightning flash and thunderstorm over East/Southeast Asia on the ENSO time scales. Atmos. Res., 169: 377–390.

Záhlava J., F. Němec, O. Santolík, I. Kolmašová, M. Parrot and C. J. Rodger. 2015. Very low frequency radio events with a reduced intensity observed by the low-altitude DEMETER spacecraft. J. Geophys. Res. Space Physics, 120(11): 9781–9794.

Zhang H., G. Lu, X. Qie, R. Jiang, Y. Fan, Y. Tian, Z. Sun, M. Liu, Z. Wang, D. Liu, G. Feng. 2016. Locating narrow bipolar events with single-station measurement of low-frequency magnetic fields. J. Atmos. Sol-terr. Phy., 143–144: 88–101.

Zhang Y., Y. Zhang, C. Li, W. Lu, D. Zheng. 2016. Simultaneous optical and electrical observations of “chaotic” leaders preceding subsequent return strokes. Atmos. Res., 170: 131–139.

Zheng D., D. R. MacGorman. 2016. Characteristics of flash initiations in a supercell cluster with tornadoes. Atmos. Res., 167: 249–264.

Zheng D., Y. Zhang, Q. Meng, L. Chen, J. Dan. 2016. Climatological comparison of small- and large-current cloud-to-ground lightning flashes over Southern China. J. Climate, 29: 2831–2848.

Zhu B., M. Ma, W. Xu, D. Ma. 2015. Some properties of negative cloud-to-ground flashes from observations of a local thunderstorm based on accurate-stroke-count studies. J. Atmos. Sol-terr. Phy., 136: 16–22.

Zhu Y., V. A. Rakov, S. Mallick, M. D. Tran. 2015. Characterization of negative cloud-to-ground lightning in Florida. J. Atmos. Sol-terr. Phy., 136: 8–15.

Reminder

Newsletter on Atmospheric Electricity presents twice a year (May and November) to the members of our community with the following information:

- ✧ announcements concerning people from atmospheric electricity community, especially awards, new books...,
- ✧ announcements about conferences, meetings, symposia, workshops in our field of interest,
- ✧ brief synthetic reports about the research activities conducted by the various organizations working in atmospheric electricity throughout the world, and presented by the groups where this research is performed, and
- ✧ a list of recent publications. In this last item will be listed the references of the papers published in our field of interest during the past six months by the research groups, or to be published very soon, that wish to release this information, but we do not include the contributions in the proceedings of the Conferences.

No publication of scientific paper is done in this Newsletter. We urge all the groups interested to submit a short text (one-page maximum with photos eventually) on their research, their results or their projects, along with a list of references of their papers published during the past six months. This list will appear in the last item. Any information about meetings, conferences or others which we would not be aware of will be welcome.

Newsletter on Atmospheric Electricity is now routinely provided on the web site of ICAE (http://www.icae.jp), and on the web site maintained by Monte Bateman http://ae.nsstc.uah.edu/.

In order to make our news letter more attractive and informative, it will be appreciated if you could include **up to two photos or figures** in your contribution!

Call for contributions to the newsletter

All issues of this newsletter are open for general contributions. If you would like to contribute any science highlight or workshop report, please contact Dr. Daohong Wang (wang@gifu-u.ac.jp) preferably by e-mail as an attached word document.

The deadline for **2016 winter** issue of the newsletter is **Nov 15, 2016**.

Editor:
Daohong Wang
President of ICAE
E-mail:wang@gifu-u.ac.jp
Tel: 81-58-293-2702
Fax: 81-58-232-1894

Compiler:
Wenjuan Zhang
Chinese Academy of Meteorological Sciences
Beijing, China
zhangwj@camscma.cn

Newsletters on Atmospheric Electricity are supported by International Commission on Atmospheric Electricity, IUGG/IAMAS.

©2016